

Chapter 6

Heat Transfer to Air-Cooled Heat Exchangers

NOTE: this chapter is written by Anthony M. Jacobi. He is the Richard W. Kritzer Distinguished Professor in the Department of Mechanical Science and Engineering at the University of Illinois at Urbana, IL 61801, USA.

ACKNOWLEDGEMENT:

The author gratefully acknowledges more than a decade of support on related topics from the Air Conditioning and Refrigeration Center (ACRC) and the Air-Conditioning and Refrigeration Technology Institute (ARTI), and respectfully acknowledges the work of collaborator Young-Gil Park, upon which this chapter heavily relies.

SUMMARY: This chapter considers heat transfer and pressure drop for refrigerant-to-air and liquid-to-air heat exchangers, with a focus on the air-side behavior. Performance correlations for flat-tube and round-tube configurations, with continuous and interrupted fins are provided.

6. 1 Introduction and Background

Most of this book is directed toward in-tube flows, and it provides the tools necessary to predict heat transfer and pressure drop for two-phase and single-phase in-tube flows. Such calculations are especially important in determining heat transfer and pressure drop for heat exchanger design and performance. However, in many vapor-compression systems as well as other applications, heat transfer to and from air is very important. Of course, some systems use water or other liquids as the heat reservoir or process stream; nevertheless, the use of air is ubiquitous and the methods for air-side calculations are different from those presented elsewhere in the book. This chapter is focused on the air-side heat transfer and pressure drop for heat exchanger analysis and design. Furthermore, because the applications motivating this chapter almost always use round-tube-and-fin or flat-tube-and-fin heat exchangers, the focus will be on those families of heat exchangers, the geometries of which are depicted schematically in Figures 6.1 and 6.2.

Air-side analysis is typically conducted using a nomenclature different from the tube-side nomenclature used throughout most of the rest of this book. While variations appear in the literature, the conventional air-side nomenclature is widely adopted, and abandoning it in this chapter would likely cause significant confusion in trying to relate the material presented here to that in the extant air-side literature. Therefore, this chapter will use a stand-alone nomenclature different from the rest of the book; the Nomenclature used in this chapter is presented in a section near the end of this chapter.

Many engineers find the widespread use of the Colburn j factor to characterize heat transfer, rather than the Nusselt number, a confusing aspect of air-side analysis. While the usage of j is probably due to early adoption in a seminal book (Kays and London, 1955), there is a theoretical basis for its use. For a steady, laminar, zero-pressure-gradient boundary layer, it can be shown through scale analysis that, except at very low Prandtl numbers, $Nu=C_1Re^{1/2}Pr^{1/3}$, where C_1 is an order-unity constant. For a steady, turbulent internal flow it is known that the heat transfer can be reasonably represented by $Nu=C_2Re^{4/5}Pr^{1/3}$, where C_2 is a constant. Motivated by boundary layer theory for laminar flows and our knowledge of turbulent flows, we form the Colburn j factor,

$$j = \frac{Nu}{RePr^{1/3}} \quad [6.1.1]$$

and anticipate heat transfer correlations will take a power-law form,

$$j = A \cdot Re^{-B} \quad [6.1.2]$$

where the constant B is likely to range from 0.2 to 0.5, depending on the nature of the flow.

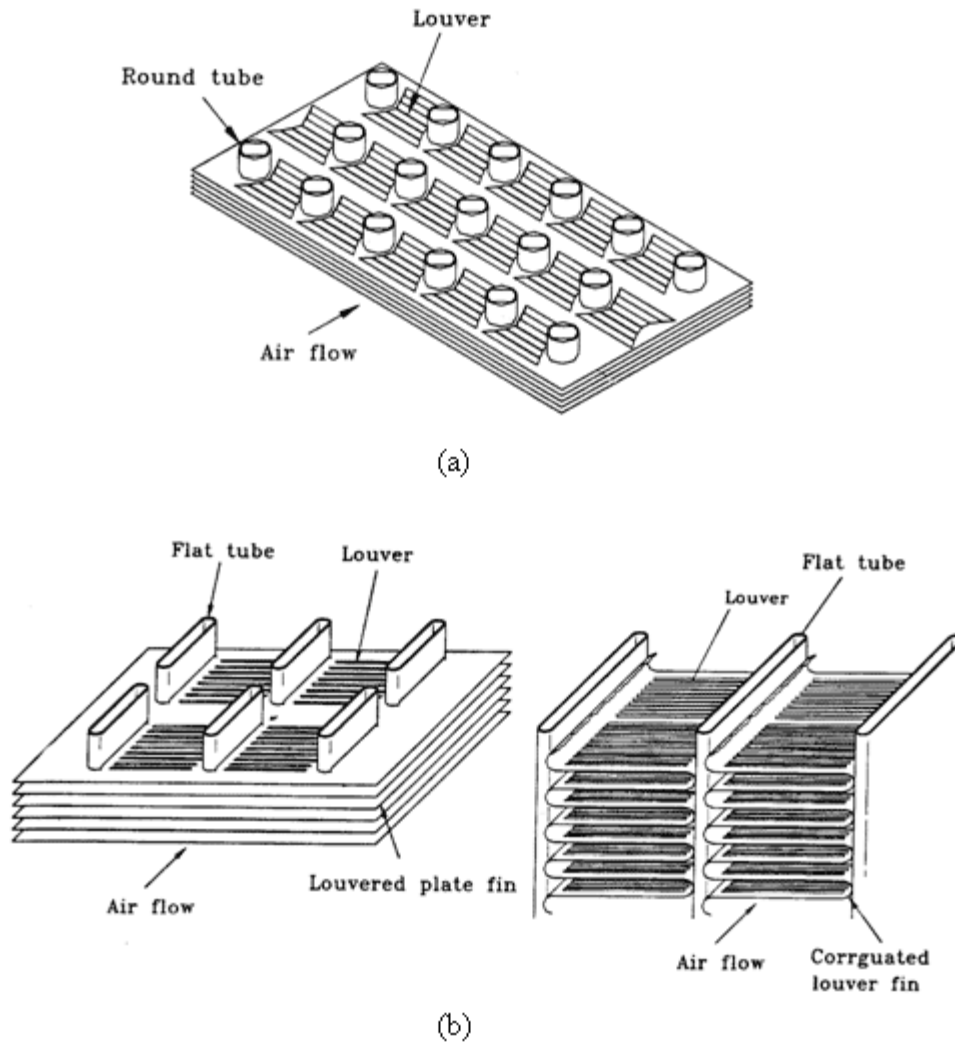


Figure 6.1 Typical fin-and-tube heat exchangers (from Wang et al., 1999a, b): (a) Round-tube heat exchanger and (b) flat-tube heat exchanger

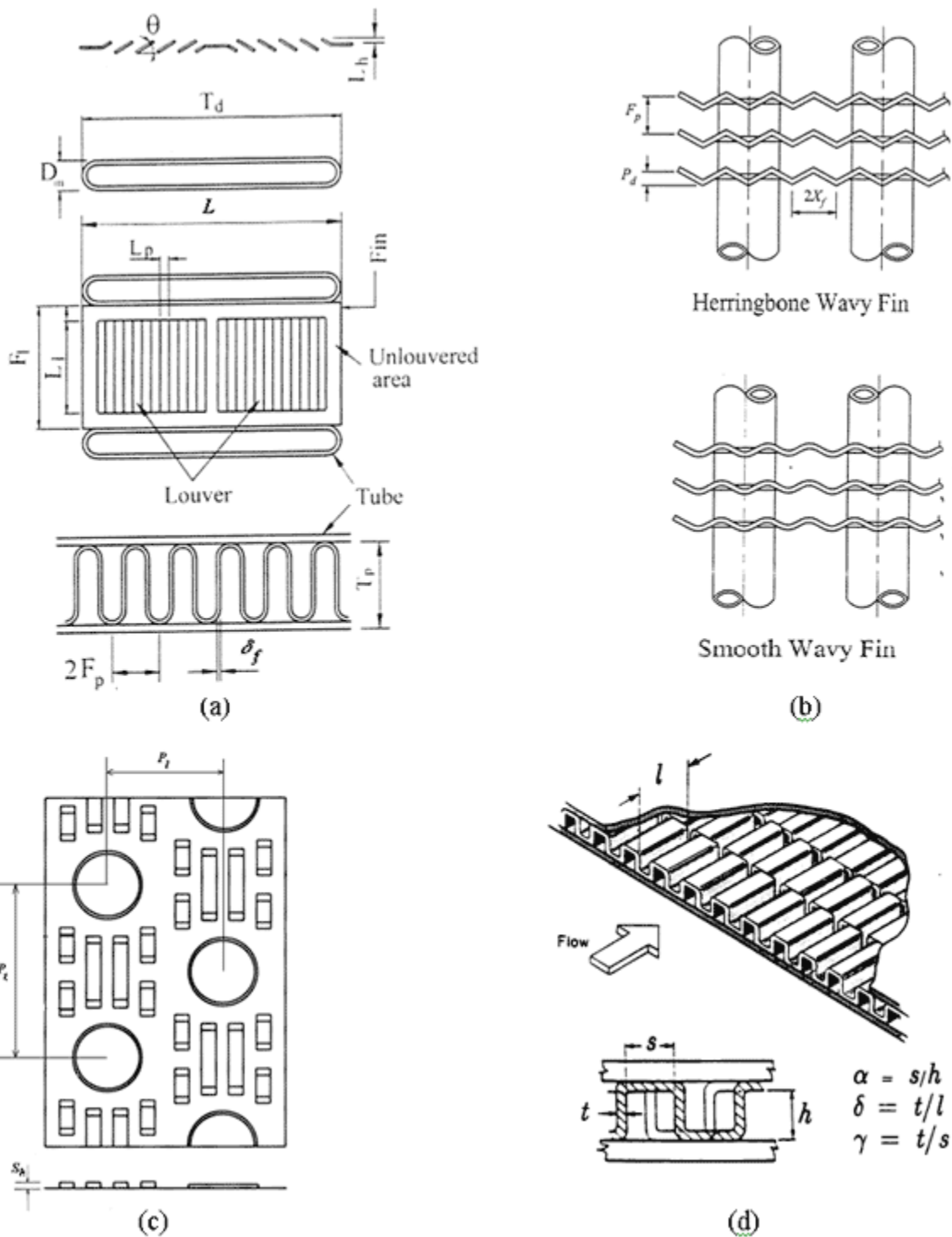


Figure 6.2 Various fin types and geometrical parameters: (a) Louvered fins (modified from Chang et al., 2000), showing a cross section of the louvers, a cross section of tube, and an end and front view of a serpentine louvered fin between two flat tubes; (b) Wavy fins (from Wang et al., 1999c), (c) Slit fins (modified from Kim and Jacobi, 2000), and (d) Rectangular offset-strip fins (from Manglik and Bergles, 1995)

For the purpose of putting forward the heat exchanger model equations in a simple form, consider single-phase flows, with two streams at steady state, and no heat leaks, an energy balance for each stream will yield

$$Q = W_a c_a (T_{a,i} - T_{a,o}) \quad [6.1.3]$$

and

$$Q = W_t c_t (T_{t,o} - T_{t,i}) \quad [6.1.4]$$

where the subscripts 'a' and 't' indicate air-side and tube-side, and 'i' and "o" indicate inlet and outlet. The equations are written for the cooling of air but could be arranged for the heating of air. Of course, if a phase change is occurring, then an energy balance can still be written in terms of mass flow rate and enthalpy change.

In addition to energy balances, the heat transfer can be characterized by a rate equation. Perhaps the most intuitive is in terms of a log-mean temperature difference (LMTD)

$$Q = UA \cdot F \cdot \Delta T_{lmcf} \quad [6.1.5a]$$

with

$$\Delta T_{lmcf} = \frac{(T_{a,i} - T_{t,o}) - (T_{a,o} - T_{t,i})}{\ln((T_{a,i} - T_{t,o}) / (T_{a,o} - T_{t,i}))} \quad [6.1.5b]$$

In Eqs. [6.1.5], the counter-flow log-mean temperature difference is used, and the correction factor F —which depends on flow geometry—is used for heat exchangers that are not in a pure counter-flow configuration. Alternatively, an effectiveness-NTU (ε - N_{TU}) approach can be used to write the rate equation

$$Q = \varepsilon \cdot (Wc)_{\min} \cdot (T_{a,i} - T_{t,i}) \quad [6.1.6a]$$

with

$$\varepsilon = f \left(\frac{UA}{(Wc)_{\min}}, \frac{(Wc)_{\min}}{(Wc)_{\max}} \right) = f(N_{TU}, C_r) \quad [6.1.6b]$$

In the ε - N_{TU} approach, the flow geometry is embodied in the relationship between ε and N_{TU} , i.e., Eq. [6.1.6b]. Whether an LMTD or ε - N_{TU} analysis is adopted, the rate equation relates heat transfer to driving potential (a ΔT) and the overall heat conductance UA , with F or $\varepsilon=f(N_{TU}, C_r)$ used to account for flow geometry in LMTD or ε - N_{TU} , respectively.

The overall conductance of the heat exchanger, UA , is the inverse of the overall thermal resistance, which is due to tube-side convection, contact and fouling resistance, tube-wall conduction resistance, and air-side convection.

$$UA = \left[\frac{1}{(\eta_o hA_T)_t} + R_{\text{contact+foul}} + R_{\text{wall}} + \frac{1}{(\eta_o hA_T)_a} \right]^{-1} \quad [6.1.7]$$

While contact and fouling resistance can be significant, a full treatment of these effects is beyond the scope of this chapter. Contact resistance depends very strongly on manufacturing methods: for brazed heat exchangers there is no contact resistance, for collared fins it is usually negligible, but for simple pressed fits it can be large (see ElSherbini *et al.* 2003). Fouling resistance depends very strongly on operating environment, history, and maintenance. Outside sources should be consulted if these effects are important (see Taborek *et al.* 1972). The conduction resistance of the tube wall is almost always negligible. Thus, for the situations to be discussed further in this chapter, Eq. [6.1.7] can be simplified to

$$UA = \frac{(\eta_o hA_T)_t \cdot (\eta_o hA_T)_a}{(\eta_o hA_T)_a + (\eta_o hA_T)_t} \quad [6.1.8]$$

In Eq. [6.1.8], the surface efficiency, η_o , depends on the fin efficiency, η_f , which in turn depends on the convection coefficient, as well as geometry, and fin material. Thus, often calculations involve iteration, and most analysis is conducted using a computer and standard software for the solution of simultaneous equations. Consider a performance calculation, in which air is cooled by the flow of water through finned tubes. If a relationship is known for the tube-side convection coefficient in terms of the water flow rate, and the air-side convection coefficient is known in terms of the air-side flow rate, then for specified flow rates and inlet temperatures, the heat transfer rate and outlet temperatures would be unknown. Calculating the heat transfer rate and outlet temperatures for this specified heat exchanger geometry constitutes a performance calculation. Analysis would proceed along the following lines: (1) calculate the convection coefficients for the specified flow rates; (2) calculate the fin efficiencies and surface efficiencies using appropriate relationships for the fin geometry (see Incropera *et al.* 2007); (3) calculate UA using Eq. [6.1.8]; finally (4) use Eqs. [6.1.3] and [6.1.4] with either [6.1.5] or [6.1.6], to simultaneously solve for Q , $T_{a,o}$ and $T_{t,o}$.

Another type of analysis is a so-called design calculation. Reconsider the problem described above, but instead of taking the heat exchanger design as fixed, take the desired heat transfer rate as specified for prescribed mass flow rates and inlet temperatures. In this case, the objective is to calculate the required heat exchanger size, UA . The calculation would follow: (1) calculate the convection coefficients for the specified flow rates; (2) calculate the fin efficiencies and surface efficiencies; then either (3a) use Eqs. [6.1.3] and [6.1.4] with the desired Q to find $T_{a,o}$ and $T_{t,o}$, then use [6.1.5] to solve for UA , or (3b) use Eqs. [6.1.6] to find UA directly from N_{tu} . Although the calculation of UA with Eq. [6.1.6] does not require outlet temperature, it may be desired to know them, and Eqs. [6.1.3] and [6.1.4] can be used for that purpose.

To this point, the discussion of air-side heat transfer has been confined to single-phase flows. Methods are presented elsewhere in this book to calculate tube-side two-phase heat transfer and pressure drop. Thus, extending the analysis to consider two-phase tube-side flows relies directly on material provided in the rest of the book. However, two-phase flows occur on the air-side as well. For example during dehumidification the air-side surface becomes wet with liquid water, and in refrigeration and heat-pumping systems the air-side surface may be subjected to frosting. A detailed discussion of the best way to represent heat exchanger performance under air-side phase-change conditions is presented by Xia and Jacobi (2005) and Park and Jacobi (2010). Analysis can be greatly complicated by fin efficiency issues (see Xia and Jacobi, 2004; Sommers and Jacobi, 2006). For conditions typical to dehumidification, an enthalpy-based approach can be adopted (see Xia and Jacobi, 2005 for restrictions):

$$Q = W_a (i_{a,i} - i_{a,o}) \quad [6.1.9]$$

$$Q = W_t (i_{t,o} - i_{t,i}) \quad [6.1.10]$$

and

$$Q = (UA / c_p) \cdot F \cdot \Delta i_{lmcf} \quad [6.1.11a]$$

with

$$\Delta i_{lmcf} = \frac{(i_{a,i} - i_{t,o}) - (i_{a,o} - i_{t,i})}{\ln((i_{a,i} - i_{t,o}) / (i_{a,o} - i_{t,i}))} \quad [6.1.11b]$$

where $i_{a,i}$ and $i_{a,o}$ are the enthalpies of moist air at the inlet and outlet of the heat exchanger, and $i_{t,i}$ and $i_{t,o}$ are the enthalpies of saturated, moist air at the tube-side inlet and outlet temperatures, respectively. Equation [6.1.11] is analogous to Eq. [6.1.5], with the log-mean enthalpy difference the driving potential for simultaneous heat and mass transfer. While the enthalpy-potential method is adequate for many air-cooling applications, it may break down for partially wet heat exchangers and will break down when mass transfer effects alter the transport coefficients.

Thus far, the focus has been on heat transfer calculations; however, in some cases these calculations are coupled to or constrained by pressure-drop calculations. In order to calculate flow rates, pressure drop, or fan power (pumping power), the friction factor must be known. By analogy to heat transfer, we might expect the friction factor will follow a power-law (see Eq. [6.1.2]):

$$f = C \cdot Re^{-D} \quad [6.1.12]$$

In many cases that expectation will be met; however, as seen later, it is overly simplistic. The friction factor can be related to flow rate and pressure drop through

$$f = \frac{A_{\min} \bar{\rho}}{A_T \rho_i} \left[\frac{2 \rho_i \Delta p}{G^2} - (K_c + 1 - \sigma^2) - 2 \left(\frac{\rho_i}{\rho_o} - 1 \right) + (1 - \sigma^2 - K_e) \frac{\rho_i}{\rho_o} \right] \quad [6.1.13]$$

where $\bar{\rho} = (\rho_i + \rho_o) / 2$, and the entrance and exit coefficients K_c and K_e are geometry dependent (see Kays and London, 1984). For air-side flows it is common that entrance and exit effects are small and density changes are negligible. For such a case, Eq. [6.1.13] simplifies to

$$f = \frac{A_{\min} \rho}{A_T} \left[\frac{2 \Delta p}{G^2} \right] \quad [6.1.14]$$

The fan power required to move the air flow through the heat exchanger is

$$P = \frac{GA_{\min} \Delta p}{\rho} \quad [6.1.15]$$

As this introductory section ends, it is worth pointing out that when an air-cooling heat exchanger is operated with a two-phase tube-side flow, such that the tube-side temperature is constant (or nearly so), then the correction factor of Eqs. [6.1.5] and [6.1.11] goes to unity; *i.e.*, $F \rightarrow 1$. Similarly, for such a case the $\varepsilon-N_{TU}$ relation of Eqs. [6.1.6] goes to $\varepsilon = 1 - \exp(-N_{TU})$.

The Air-Conditioning and Refrigeration Technology Institute (ARTI) sponsored research in the early 2000's to review and advance the state of the art in air-side heat transfer. Much of what is reported in the following section is derived from that work (see Jacobi *et al.*, 2001; 2005).

6.2 Performance of plain-fin, round-tube heat exchangers

Rich (1973) and Wang *et al.* (1996) reported that heat transfer and friction factors do not depend strongly on fin spacing. Gray and Webb (1986) provided a j -factor correlation independent of fin spacing but a friction correlation with f increasing as fin spacing decreased. Yan and Sheen (2000) concluded that both heat transfer and pressure drop increase as fin spacing decreases, for a fin spacing from 2.0 to 1.4 mm. Disagreement in the literature as to the effect of fin spacing may be due to geometrical variation and experimental uncertainties; however, most investigators conclude that f is higher for a smaller fin spacing and j is relatively independent of fin spacing. It is also generally accepted that at low Re the j -factor decreases as the number of tube rows increases and j is insensitive—or might increase slightly—with the number of tube rows at high Re , with the friction factor generally insensitive to tube rows (see Rich, 1975; Yan and Sheen, 2000; and Abu Madi *et al.* 1998). A staggered tube arrangement is generally preferred over an in-line arrangement, because wake effects are reduced by the staggered-tube geometry. Recent work on enhancing plain-fin performance using vortex generators has been reported (ElSherbini and Jacobi, 2002; Sommers and Jacobi, 2005; and Joardar and Jacobi, 2007, 2008).

When the heat exchanger is operated under wet-surface conditions, such as in dehumidifying applications, the retained condensate on the air-side surface changes the surface geometry and the airflow pattern and can increase surface heat transfer resistance. McQuiston (1978a) found both heat transfer and friction to increase of under wet conditions and reported that j is higher for dropwise condensation than filmwise condensation. While most investigators agree that f increases under wet conditions, there is not uniform agreement that j increases. Wang and co-workers (1997a) found j decreases under wet conditions at low Reynolds numbers ($Re_{Dc} < 2000$), and is nearly the same or slightly higher than for dry conditions at higher Reynolds numbers. Guillory and McQuiston (1973) had earlier proposed that condensate on a smooth fin is akin to increasing surface roughness, and Tree and Helmer (1976) used this view to explain enhanced heat transfer at high Reynolds numbers as due to a transition to turbulence. Finding that the increase of j under wet conditions was insignificant at a very low Reynolds numbers, McQuiston (1978a) also supports this rather simple surface-roughness model. Jacobi and Goldschmidt (1990) found that condensate retained as inter-fin bridges at low Reynolds numbers has detrimental effect on heat transfer. In an experimental study of condensate drainage characteristics, perhaps the first in which retained mass of condensate was measured along with thermal-hydraulic performance, Korte and Jacobi (2001) showed that the mass of retained condensate decreases as air velocity increases, and condensate can degrade heat transfer by occupying surface area and blocking airflow. Due to decreased retention at high velocities both j and f under wet conditions differ from those of dry conditions by less at higher Reynolds numbers for the plain-fin-and-tube heat exchanger.

On the basis of experimental data from 3 heat exchangers with the fin spacing from 2.0 to 3.0 mm, Wang *et al.* (1997a) reported fin spacing to be unimportant to both f and j under dehumidifying conditions. To the contrary, Korte and Jacobi (2001) reported sensible heat transfer and pressure drop dependent on fin

spacing and contact angle*. They conducted experiments with heat exchangers having 14 tube rows and a fin spacing from 2.12 to 6.35 mm. Some heat exchangers were coated and had a 45° average contact angle, while others without a coating or with an anti-corrosion coating had contact angles of 60° to 75°. One specimen with a 6.35 mm fin spacing and a 75° contact angle showed an enhanced j under wet conditions, but a similar sample with a 3.18 mm fin spacing showed no clear trend in j . For these heat exchangers with relatively large fin spacing, Korte and Jacobi did not find the sensible j to decrease under wet conditions, as reported by others for heat exchangers with a small fin pitch. They found that f was higher under wet conditions than for dry conditions for heat exchangers with a small fin spacing, but wet- and dry-surface f factors differed by less than the experimental uncertainty for large fin spacing. The fin spacing effect depended on the contact angle—the increase of f under wet conditions was greater for small fin spacing and large contact angles.

The effect of the number of tube rows under wet conditions is similar to that under dry conditions. Wang *et al.* (1996) reported that j decreased as the number of tube rows increased and this effect was stronger for a smaller fin spacing, but they found f to be independent of fin spacing (see also Wang *et al.* 1997a).

Wang *et al.* (1997a) reported that the effect of relative humidity on f is negligible for plain-fin, round-tube heat exchangers under fully wet conditions, and that j is almost independent of relative humidity. Another report by Wang and Chang (1998) reached similar conclusions on the negligible effect of relative humidity on j , but their data indicated an effect on f for some conditions. They suggest that f is sensitive to relative humidity because the flow path becomes narrower with a thicker water film at higher humidity. Wang *et al.* (1997a) reduced their experimental data using the fin efficiency calculation method of Threlkeld (1970) to conclude the j -factor independence from relative humidity, but they reported that the j showed a decrease with relative humidity if they use the calculation method of McQuiston and Parker (1994). An article on wet-fin-efficiency calculation methods by Wu and Bong (1994) discussed these fin efficiency calculation methods and supported the method by Threlkeld (1970), based on enthalpy as the driving potential. Recent work by Xia and Jacobi (2005) reviews data reduction methods and suggests a consistent LMTD approach that may be preferred, especially for partially wet surfaces. The effect of relative humidity on j factor under fully wet surface conditions is negligible. Discrepancies on the effect of relative humidity found in the literature can probably be attributed to the differences in wet-fin-efficiency calculation method.

Most heat exchanger performance studies of wet-surface conditions consider only fully wet surfaces, but a partially wet condition can occur in application. For partially wet conditions, it is necessary to consider the dry- and wet-surface fin area separately for proper fin efficiency calculation; a method for accomplishing this is discussed by Park and Jacobi (2010).

6.3 Performance of louvered-fin, round-tube heat exchangers

Fin spacing has a small effect on j and f (See Chang *et al.* 1995); Wang *et al.* (1998) reported that j decreases as fin spacing decreases for $Re_{Dc} < 1000$ and j is independent of fin pitch for $Re_{Dc} > 1000$. The effect of fin spacing on f factor was found to be small compared to the case of plain-fin heat exchangers. Reflecting this dependence of j on Reynolds number, Wang *et al.* (1999a) provided two separate j factor

* **Contact angle** – A measure of surface wettability defined as the maximum or minimum angle between liquid-gas contact line and liquid-solid contact line measured before the liquid-gas interface starts to move. The maximum angle is called as ‘advancing contact angle (θ_A)’ and the minimum as ‘receding contact angle (θ_R).’

correlations, each applicable in a particular Reynolds number range. Yan and Sheen (2000) reported no discernable trends in j with fin pitch in their experimental results, and f factor increases for smaller fin spacing. As for the plain-fin geometry, heat transfer decreases as the number of tube rows increases for $Re_{Dc} < 3000$ and friction factor is independent of the number of tube rows (Chang *et al.* 1995). Wang *et al.* (1998) also reported that f factor is nearly independent of number of tube rows. They observed that the j factor decreases with a larger number of tube rows for $Re_{Dc} < 2000$, and j is independent of tube rows for $Re_{Dc} > 2000$. Yan and Sheen (2000) found a similar result. Wang *et al.* (1998) explained that the degradation of heat transfer at low Reynolds numbers is due to the effect of thermal wakes downstream of the tubes, which is more detrimental to a heat exchanger with larger number of tube rows because it has a longer airflow depth. Wang *et al.* (1998) argued that the dependence of j factor on the number of tube rows disappears at high Reynolds numbers when the downstream eddies from the tubes and the turbulence mixing enhance the heat transfer.

Air-side friction decreases for a smaller tube diameter as reported by Wang *et al.* (1998). They reported that heat transfer decreases for a larger tube diameter at low Reynolds numbers, because the ineffective downstream region is greater for a larger tube. They reported that the effect of tube size disappears for high Reynolds numbers due to the turbulent mixing. Fu *et al.* (1995) found the j factor independent of the fin spacing under dry surface conditions, but for wet conditions the sensible j factor decreases with a smaller fin spacing for $Re_{Dc} < 2000$, and j is independent of fin spacing for $Re_{Dc} > 2000$. The f factor increases for a smaller fin spacing. These findings are buttressed by the work of Wang *et al.* (2000), who also reported a relatively small effect of the number of tube rows on f and j factors under wet conditions.

Wang and Chang (1998) reported that the sensible heat transfer coefficient is independent of relative humidity. They also suggested that the heat transfer enhancement due to louvers or slit-fins becomes negligible under wet conditions for a frontal air velocity lower than 0.7 m/s, implying the decrease in sensible heat transfer coefficient due to condensation is greater for interrupted fins than for plain fins. Based on their experimental data, they concluded that a hydrophilic coating decreases pressure drop but does not affect sensible heat transfer (See also Liu and Jacobi, 2009). Kim and Jacobi (2000) found a similar effect of coating on slit-fin heat exchangers. Fu *et al.* (1995) drew different conclusions on the effect of relative humidity on f and j factors. They reported that j decreases and f increases for a higher relative humidity. Reflecting on the issue of wet-fin-efficiency calculation method as discussed by Wang *et al.* (1997a), the dependence of j factor on relative humidity is probably because they used McQuiston's fin efficiency calculation method. Wang *et al.* (2000) reported a relatively small effect of relative humidity on j factor and a slight increase of pressure drop for a higher humidity. Since the condensation mode* is a crucial parameter that depends on the surface contact angles, generalized conclusions about the effects of relative humidity on heat exchanger performance should be made with a careful consideration of surface condition.

6.4 Performance of slit-fin, round-tube heat exchanger

Fin spacing may have a stronger effect on slit-fin heat exchangers than louvered-fin heat exchangers (Wang *et al.* 1999b). From their experiments on 12 slit-fin test samples under dry conditions, both heat transfer coefficient and pressure drop decreased as fin spacing increased.

* **Condensation mode** – A geometrical distinction of how condensate is retained on local surface area. Based on the shape of condensate, there are ‘dropwise’ and ‘filmwise’ condensation modes that depend on surface contact angles.

As with the other geometries, there is a relatively small effect of the number of tube rows on friction factor and a decreased j factor for an increasing number of tube rows (Wang *et al.* 1999b). However, Wang and co-workers observed a different j factor behavior when there were more than 4 tube rows and the fin spacing was small. Contrary to the general trends that j decreases with Reynolds number, j increases to a peak and decreases with Reynolds number for a large number of tube rows. Du and Wang (2000) also reported that the number of tube rows has little effect on f factor, and that j factor decreases significantly with increasing number of tube rows for $Re_{Dc} < 1000$ and is independent of tube rows for $Re_{Dc} > 2000$.

Kim and Jacobi (2000) investigated the thermal-hydraulic performance and condensate retention characteristics of slit-fin heat exchangers through experiments on 24 test samples with fin spacing 1.3, 1.5 and 1.7 mm. They found f to increase and j to decrease for smaller fin spacing under wet conditions. Since retained condensate can easily form bridges between fins with a smaller spacing, this result might be due to condensate retention. Under dry conditions 2-row slit-fin heat exchangers had a lower f and a higher j factor than 3-row heat exchangers; whereas, under wet conditions, 2-row exchanger had a higher f than did a 3-row specimen. Kim and Jacobi (2000) reported that retained condensate per unit surface area decreases with a larger number of tube rows, and they attributed this to a ‘sweeping effect’ of condensate drops in the airflow direction. A surface with a hydrophilic coating consistently decreased air-side pressure drop under wet conditions, but the effect of the coating on j factor under wet conditions was not clear in their results.

6.5 Performance of wavy-fin, round-tube heat exchanger

Many articles about wavy-fin heat exchangers include both staggered and inline tube layout, and the results depend on tube layout. Wang *et al.* (1997b) reported that j is nearly independent of fin spacing and f shows a cross-over with Reynolds number. For $Re_{Dc} < 1000$, f decreases with larger fin spacing, and for $Re_{Dc} > 1000$, f increases with larger fin spacing. Abu Madi *et al.* (1998) reported that friction is not influenced by fin thickness, and heat transfer coefficient increases for a smaller fin thickness.

Wang *et al.* (1997b) reported that friction factor is independent of the number of tube rows for both inline and staggered-tube layouts. For inline tube samples, they reported that the effect of tube rows on j is similar to interrupted-fin heat exchangers; for $Re_{Dc} < 2000$, j decreases as the number of tube rows increases, and for $Re_{Dc} > 2000$, j is independent of the number of tube rows. In staggered-tube heat exchangers, j factor dependence on tube rows is quite different from inline cases; for $Re_{Dc} < 900$, j decreases slightly with more tube rows, and for $Re_{Dc} > 900$, j increases with more tube rows. Wang *et al.* explained that the thermal boundary layer along continuous wavy fins grows at low Reynolds numbers, and it degrades heat transfer more for longer flow depth by larger number of tube rows. However, as the Reynolds number increases the thermal boundary layer is broken as the airflow is driven by wave patterns, and the effect of thermal boundary layer diminishes. This explanation is consistent with the flow visualization work of Rush *et al.* (1999). They explained the difference in j by tube layouts by arguing that only the staggered-tube layout has the enhancement of heat transfer by downstream turbulence. Kim *et al.* (1997) compared the effect of tube layout and fin pattern on the performance of wavy-fin heat exchangers. They reported that herringbone wavy fins have higher heat transfer than smooth wavy fins. However the area goodness factor (j/f) of smooth type was higher, which means higher friction with herringbone type. They also reported that staggered-tube layout gives higher heat transfer than inline layout.

Wang *et al.* (1999c) investigated the effect of geometrical parameters on the performance of herringbone wavy fin heat exchangers under wet conditions. They found that the effects of fin pitch on f and j factors

depend on the number of tube rows; f decreases as fin pitch increases, and this effect is stronger for 6-row coils than single-row coils. As fin pitch increases, sensible j factor increases for 6-row coils and decreases for 1-row coils. The effect of tube rows on the herringbone wavy-fin heat exchangers under wet conditions has unique behavior in f : as the number of tube rows increases, f decreases unlike other fin geometries. However, sensible j factor, like other fin geometries, decreases with an increasing number of tube rows for small fin pitches and low Reynolds numbers. Wang and co-workers also reported effects of tube diameter combined with fin pitch and number of tube rows, but their conclusions about tube diameter need to be carefully examined since their plots with different tube diameters also involved different wave depths.

6.6 Performance of louvered-fin, flat-tube heat exchanger

Although some flat-tube, louvered-fin heat exchangers are built with louvered plate fins and multiple tube rows, most have serpentine louvered fins with a single-row of flat-tubes. Serpentine louvered-fin, flat-tube heat exchangers are often used in applications where compactness is highly valued. The flat-tube design offers advantages with respect to the flow through the louver bank being normal to the louver bank, as well as the elimination of the tube wake caused by a round tube, and reduced form drag on the tubes. Compound enhancement of louver-fin heat exchangers has been reported by Joardar and Jacobi (2005).

While tube diameter is used as the characteristic length for round-tube heat exchangers, the louver pitch is usually used as the characteristic length for flat-tube heat exchangers. Fin pitch is important for both round and flat tube geometries, but tube diameters and pitches become less relevant to flat-tube heat exchanger performance and instead, louver pitch, louver length, louver angle and fin thickness have more influence. The performance of louvered-fin heat exchangers is similar to that of offset-strip fin heat exchangers, with boundary-layer re-starting as an important enhancement mechanism (see DeJong and Jacobi, 1996; DeJong et al. 1998; DeJong and Jacobi 2003a,b). Davenport (1983) described the physical significance of the ratio of louver length to fin length, and later Osada *et al.* (1999) found it to be an important parameter in condensate drainage under wet conditions. Achaicha and Cowell (1988) found j independent of Re , for $Re_{Dh} < 300 \sim 1000$ which they explained as being because the airflow is relatively duct directed at a low Re and louver directed at a high Re (see Webb and Trauger 1991). The effects of individual design parameters is most easily studied through the available correlations for j and f ; well-established correlations are provided by Chang and Wang (1997) and Chang *et al.* (2000); the most complete and comprehensive is that provided by Park and Jacobi (2009a).

Early work on wet-surface heat transfer by McLaughlin and Webb (2000a,b) and Kaiser and Jacobi (2000) was followed by an extensive study by Jacobi and co-workers (see Jacobi et al. 2005). The most complete correlation for performance is that provided by Park and Jacobi (2009b), with a method for handling partially wet surfaces described by Park and Jacobi (2010). Some limited work has also been reported for the louvered-fin, flat-tube geometry under frosted-surface conditions (see Xia and Jacobi, 2004; Xia *et al.* 2006; and Xia and Jacobi, 2010).

6.7 Performance of slit-fin, flat-tube heat exchanger

In practice this fin is not implemented as serpentine fins but rectangular offset fins attached to flat tubes. A number of performance correlations are available for this geometry, most notably that of Manglik and Bergles (1995), which has been recently extended to very high Re by Michna *et al.* (2007). Kaiser and Jacobi (2000) studied two automotive evaporators with serpentine slit fins under wet conditions and

reported the slit-fin geometry superior to louvered-fin in condensate drainage, but no thermal-hydraulic data were reported. A compound enhancement of slit fins using vortex generators was reported by Smotrýs *et al.* (2003).

6. 8 Predicting Air-Side Thermal-Hydraulic Performance

Selecting performance correlations for round-tube heat exchangers. Round-tube heat exchangers with plain fins have been studied for decades, and many correlations are available. That of Gray and Webb (1986) is well established; it was modified and extended by Wang and Chang (1998) to include a broader set of data, and that correlation and f factor correlation by Wang *et al.* (1996) are useful, because of the wide range of parameters covered. In order to enhance generality, the correlations by Abu-Madi *et al.* (1998) may be useful, because the provided limits of the intermediate non-dimensional parameters (R_1 to R_9) reduce the possibility of applying an unreasonable combination of parameters. For plain-fin, round-tube heat exchangers under wet conditions, the correlations by Wang *et al.* (1997a) covers a broad range of designs and provide good predictions. The nature of the frosting condition makes a true steady state measurement impossible; however, Emery and Siegel (1990) provide correlations based on a single test sample, and application is limited. Nevertheless, these correlations have a sound physical basis.

There are many reports available in the literature for the louvered-fin, round-tube geometry. Correlations by Wang *et al.* (1999a) and Wang *et al.* (2000) are good for dry and wet conditions, respectively. These correlations span a wide range of parameters and have good agreement with experimental data.

For slit-fin, round-tube heat exchangers under dry conditions, the j and f factor correlations by Wang *et al.* (1999b) are probably the most complete. For wet-surface conditions, the correlations by Kim and Jacobi (2000) appear to be the only ones available for slit-fin, round-tube heat exchangers. The parameter space of the correlations by Kim and Jacobi (2000) is similar to that of Wang *et al.* (1999b), but the range is smaller. Correlations for frosting conditions are not available in the open literature for slit, louver and wavy-fin exchangers. For round-tube heat exchangers with wavy fins, the correlations by Wang *et al.* (1997b) and Wang *et al.* (1999c) are good for dry and wet conditions, respectively.

Selecting performance correlations for flat-tube heat exchangers. For flat-tube louver-fin heat exchangers, Wang *et al.* (1996) and Chang *et al.* (2000) provide good correlations using a database from 91 heat exchangers operating with dry-surface conditions. That work was extended to include the work of others, along with new data by Park and Jacobi (2009a,b), and to include partially wet-surface conditions by Park and Jacobi (2010). For a slit-fin geometry, the j and f factor correlations for dry conditions by Manglik and Bergles (1995) are most widely accepted. Due to the substantial difference in geometry from other flat-tube heat exchangers, parameters only relevant to this geometry are used in the correlations. Wet and frosting conditions are not found in the literature for this geometry.

Table 6.1 Heat Exchanger Correlations

Table 6.1 Heat Exchanger Correlations: Round Tube				
Fin type	Surface condition	Author (year)	Correlations	Range of parameters / Comments
Plain	Dry	Wang <i>et al.</i> (1996)	<u>j – factor correlation</u> $j_4 = 0.14 \text{Re}_{D_c}^{-0.328} \left(\frac{P_t}{P_l} \right)^{-0.502} \left(\frac{F_p}{D_c} \right)^{0.0312}$ $\frac{j_N}{j_4} = 0.991 \left[2.24 \text{Re}_{D_c}^{-0.092} \left(\frac{N}{4} \right)^{-0.031} \right]^{0.607(4-N)}$	* Modified from Gray & Webb (1986) Parameters $\text{Re}_{D_c} = 300 \sim 8000$ $D_o = 7 \sim 19.51\text{mm}$ $F_p = 1.07 \sim 8.51\text{mm}$ $N = 1 \sim 8$ (staggered) $P_t = 20.35 \sim 50.73\text{mm}$ $P_l = 12.7 \sim 44.09\text{mm}$
Plain	Dry	Wang <i>et al.</i> (1996)	<u>f – factor correlation</u> $f = 1.039 \text{Re}_{D_c}^{-0.418} \left(\frac{\delta_f}{D_c} \right)^{-0.104} N^{-0.0935} \left(\frac{F_p}{D_c} \right)^{-0.197}$	Parameters $\text{Re}_{D_c} = 800 \sim 7500$ $D_c = 10.51\text{mm}$ $F_p = 1.77 \sim 3.21\text{mm}$ $N = 2 \sim 6$ (staggered) $P_t = 25.4\text{mm}$ $P_l = 22\text{mm}$

Table 6.1 Heat Exchanger Correlations: Round Tube

Fin type	Surface condition	Author (year)	Correlations	Range of parameters / Comments
Plain	Dry	Abu-Madi <i>et al.</i> (1998)	<p><u>j & f – factor correlations</u></p> $j_4 = \text{Re}^{-0.44} R_4^{-3.07} R_{5,1}^{0.37} R_7^{-6.14} R_9^{-2.13}$ $\frac{j_4}{j_N} = 0.87 + 0.0000143 \text{Re}^{0.55} N^{-0.67} R_3^{-3.13} R_{5,1}^{4.95}$ $f = \text{Re}^{-0.25} R_4^{-1.43} R_{5,1}^{1.37} R_8^{1.65} R_9^{-3.05}$ <p>where,</p> $R_3 = \frac{D_o}{D_i} \left(1 - \frac{\delta_f}{F_p} \right) + 2 \frac{P_t P_l}{\pi D_i F_p} - \frac{D_o^2}{2 D_i F_p} + \frac{2 \delta_f P_t}{\pi D_i F_p N} \quad R_4 = \frac{F_p P_t}{(P_t - D_o)(F_p - \delta_f)}$ $R_5 = \frac{\pi N D_o \left(1 - \frac{\delta_f}{F_p} \right)}{P_t} + \frac{N}{F_p} \left(2 P_l - \frac{\pi D_o^2}{2 P_t} + \frac{2 \delta_f}{N} \right); \quad R_{5,1} = \frac{R_5}{N}$ $R_6 = \frac{4 P_l N}{R_5}; \quad R_7 = \frac{1}{1 + \frac{2 \pi D_o (F_p - \delta_f)}{4 P_t P_l - \pi D_o^2 + \frac{4 P_t \delta_f}{N}}}$ $R_8 = \frac{F_p}{D_o}; \quad R_9 = \frac{P_l}{D_o}$	<p>Parameters</p> $\text{Re}_{D_h} = 200 \sim 6000$ $D_o = 9.956 \text{mm}$ $\delta_f = 0.12 \sim 0.13 \text{mm}$ $F_p = 1.64 \sim 2.65 \text{mm}$ $N = 1 \sim 4$ (staggered) $P_t = 19 \sim 25.4 \text{mm}$ $P_l = 16 \sim 22 \text{mm}$
				<p>Limits</p> $R_3 = 7.26 \sim 19.3$ $R_4 = 1.77 \sim 2.25$ $R_{5,1} = 11.0 \sim 21.8$ $R_7 = 0.86 \sim 0.95$ $R_8 = 0.16 \sim 0.27$ $R_9 = 1.60 \sim 2.21$

Table 6.1 Heat Exchanger Correlations: Round Tube

Fin type	Surface condition	Author (year)	Correlations	Range of parameters / Comments
Plain	Wet	Wang <i>et al.</i> (1997a)	<p><u>j & f – factor correlations</u></p> $j_4 = 0.29773 \text{Re}_{D_c}^{-0.364} \varepsilon^{-0.168}$ $j_N = 0.4 \text{Re}_{D_c}^{-0.468+0.04076N} \varepsilon^{0.159} N^{-1.261}$ $f = 28.209 \text{Re}_{D_c}^{-0.5653} N^{-0.1026} \left(\frac{F_p}{D_c}\right)^{-1.3405} \varepsilon^{-1.3343}$ <p>where, $\varepsilon = \frac{A_{tot}}{A_{tube}}$</p>	<p>Parameters</p> $\text{Re}_{D_c} = 400 \sim 5000$ $D_c = 10.23\text{mm}$ $\delta_f = 0.13\text{mm}$ $F_p = 1.82 \sim 3.20\text{mm}$ $N = 2 \sim 6$ (staggered) $P_t = 25.4\text{mm}$ $P_l = 22\text{mm}$ $T_{dry,in} = 27^\circ\text{C}$ RH = 50~90%
Plain	Frosted	Emery & Siegel (1990)	<p>Frosted-to-dry ratios</p> $\frac{\Delta P_{fr}}{\Delta P_{dry}} = 1.00 + 10.24 \left(\frac{M_{frost}}{A_{tot}}\right) + 79.55 \left(\frac{M_{frost}}{A_{tot}}\right)^2$ $\frac{h_{a,fr}}{h_{a,dry}} = 1.00 - 1.118 \cdot 10^3 \Delta w + 8.14 \cdot 10^5 \Delta w^2 - 2.11 \cdot 10^8 \Delta w^3$ <p>Δw: Difference of specific humidity between free stream and fin surface</p> <p><u>j & f – correlations for dry condition</u></p> $j = 0.00917(\text{Re}_{Dh}/1000)^{-0.313}$ $f = 0.0398(\text{Re}_{Dh}/1000)^{-0.055}$	<p>* Based on single coil data</p> <p>Parameters</p> $D_o = 19.3\text{mm}$ $P_l = 44.0\text{mm}$ $P_t = 51.0\text{mm}$ $L = 510\text{mm}$ $F_p = 6.35\text{mm}$ $\delta_f = 0.51\text{mm}$

Table 6.1 Heat Exchanger Correlations: Round Tube

Fin type	Surface condition	Author (year)	Correlations	Range of parameters / Comments
Louver	Dry	Wang <i>et al.</i> (1999a)	<p><u>j – factor correlation</u></p> <p>For $Re_{D_c} < 1000$,</p> $j = 14.3117 Re_{D_c}^{J1} \left(\frac{F_p}{D_c}\right)^{J2} \left(\frac{L_h}{L_p}\right)^{J3} \left(\frac{F_p}{P_t}\right)^{J4} \left(\frac{P_t}{P_t}\right)^{-1.724}$ <p>where,</p> $J1 = -0.991 - 0.1055 \left(\frac{P_t}{P_t}\right)^{3.1} \ln\left(\frac{L_h}{L_p}\right)$ $J2 = -0.7344 + 2.1059 \left(\frac{N^{0.55}}{\ln(Re_{D_c}) - 3.2}\right)$ $J3 = 0.08485 \left(\frac{P_t}{P_t}\right)^{-4.4} N^{-0.68}$ $J4 = -0.1741 \ln(N)$ <p>For $Re_{D_c} \geq 1000$,</p> $j = 1.1373 Re_{D_c}^{J5} \left(\frac{F_p}{P_t}\right)^{J6} \left(\frac{L_h}{L_p}\right)^{J7} \left(\frac{P_t}{P_t}\right)^{J8} (N)^{0.3545}$ <p>where,</p> $J5 = -0.6027 + 0.02593 \left(\frac{P_t}{D_h}\right)^{0.52} (N)^{-0.5} \ln\left(\frac{L_h}{L_p}\right)$ $J6 = -0.4776 + 0.40774 \left(\frac{N^{0.7}}{\ln(Re_{D_c}) - 4.4}\right)$	<p>Parameters</p> <p>$Re_{D_c} = 300 \sim 7000$</p> <p>$F_p = 1.21 \sim 2.49mm$</p> <p>$D_c = 6.93 \sim 10.42mm$</p> <p>$P_t = 17.7 \sim 25.4mm$</p> <p>$P_l = 12.7 \sim 19.05mm$</p> <p>$L_h = 0.79 \sim 1.4mm$</p> <p>$L_p = 1.7 \sim 3.75mm$</p> <p>$N = 1 \sim 6$ (staggered)</p> <p>Uncertainties</p> <p>j – 95.5% data within 15%</p> <p>f – 90.8% data within 15%</p>

Table 6.1 Heat Exchanger Correlations: Round Tube

Fin type	Surface condition	Author (year)	Correlations	Range of parameters / Comments
Louver	Dry	Wang <i>et al.</i> (1999a)	$J7 = -0.58655 \left(\frac{F_p}{D_h} \right)^{2.3} \left(\frac{P_l}{P_t} \right)^{-1.6} N^{-0.65}$ $J8 = 0.0814 (\ln(\text{Re}_{D_c}) - 3)$ $D_h = \frac{4A_{\min} L}{A_{\text{tot}}}$ <p><u>f – factor correlation</u></p> <p>For N=1,</p> $f = 0.00317 \text{Re}_{D_c}^{F1} \left(\frac{F_p}{P_l} \right)^{F2} \left(\frac{D_h}{D_c} \right)^{F3} \left(\frac{L_h}{L_p} \right)^{F4} \left(\ln \left(\frac{A_{\text{tot}}}{A_{\text{tube}}} \right) \right)^{-6.0483}$ <p>where,</p> $F1 = 0.1691 + 4.4118 \left(\frac{F_p}{P_l} \right)^{-0.3} \left(\frac{L_h}{L_p} \right)^{-2} \left(\ln \left(\frac{P_l}{P_t} \right) \right) \left(\frac{F_p}{P_t} \right)^3$ $F2 = -2.6642 - 14.3809 \left(\frac{1}{\ln(\text{Re}_{D_c})} \right)$ $F3 = -0.6816 \ln \left(\frac{F_p}{P_l} \right)$ $F4 = 6.4668 \left(\frac{F_p}{P_t} \right)^{1.7} \ln \left(\frac{A_{\text{tot}}}{A_{\text{tube}}} \right)$	

Table 6.1 Heat Exchanger Correlations: Round Tube

Fin type	Surface condition	Author (year)	Correlations	Range of parameters / Comments
Louver	Dry	Wang <i>et al.</i> (1999a)	For $N > 1$, $f = 0.06393 \text{Re}_{Dc}^{F5} \left(\frac{F_p}{D_c}\right)^{F6} \left(\frac{D_h}{D_c}\right)^{F7} \left(\frac{L_h}{L_p}\right)^{F8} N^{F9} (\ln(\text{Re}_{Dc}) - 4.0)^{-1.093}$ where, $F5 = 0.1395 - 0.0101 \left(\frac{F_p}{P_l}\right)^{0.58} \left(\frac{L_h}{L_p}\right)^{-2} \left(\ln\left(\frac{A_{tot}}{A_{tube}}\right)\right) \left(\frac{P_l}{P_t}\right)^{1.9}$ $F6 = -6.4367 \left(\frac{1}{\ln(\text{Re}_{Dc})}\right)$ $F7 = 0.07191 \ln(\text{Re}_{Dc})$ $F8 = -2.0585 \left(\frac{F_p}{P_t}\right)^{1.67} \ln(\text{Re}_{Dc})$ $F9 = 0.1036 \left(\ln\left(\frac{P_l}{P_t}\right)\right)$	

Table 6.1 Heat Exchanger Correlations: Round Tube

Fin type	Surface condition	Author (year)	Correlations	Range of parameters / Comments
Louver	Wet	Wang <i>et al.</i> (2000)	<p><u>j – factor correlation</u></p> $j = 9.717 \text{Re}_{Dc}^{J1} \left(\frac{F_p}{D_c}\right)^{J2} \left(\frac{P_t}{P_t}\right)^{J3} \ln\left(3 - \frac{L_p}{F_p}\right)^{0.07162} N^{-0.543}$ <p>where,</p> $J1 = -0.023634 - 1.2475 \left(\frac{F_p}{D_c}\right)^{0.65} \left(\frac{P_t}{P_t}\right)^{0.2} N^{-0.18}$ $J2 = 0.856 \exp(\tan \theta)$ <p style="text-align: center;">→ louver angle: $\theta = \sin^{-1}(L_h / L_p)$</p> $J3 = 0.25 \ln(\text{Re}_{Dc})$ <p><u>f – factor correlation</u></p> $f = 2.814 \text{Re}_{Dc}^{F1} \left(\frac{F_p}{D_c}\right)^{F2} \left(\frac{P_t}{D_c}\right)^{F3} \left(\frac{P_t}{P_t} + 0.091\right)^{F4} \left(\frac{L_p}{F_p}\right)^{1.958} N^{0.04674}$ <p>where,</p> $F1 = 1.223 - 2.857 \left(\frac{F_p}{D_c}\right)^{0.71} \left(\frac{P_t}{P_t}\right)^{-0.05}$ $F2 = 0.8079 \ln(\text{Re}_{Dc})$ $F3 = 0.8932 \ln(\text{Re}_{Dc})$ $F4 = -0.999 \ln\left(\frac{2\Gamma}{\mu_f}\right)$ <p style="text-align: center;">•</p> $\Gamma = \frac{m}{WN} : \text{condensate flow rate per unit width per tube row}$ <p>μ_f : dynamic viscosity of water</p>	<p>Parameters</p> $\text{Re}_{Dc} = 400 \sim 3000$ $P_t = 25.4 \text{mm}$ $P_l = 19 \sim 22 \text{mm}$ $D_c = 10.33 \text{mm}$ $F_p = 1.2 \sim 2.5 \text{mm}$ $\theta = 24.4 \sim 28.2^\circ$ $N = 1 \sim 2$ (staggered) $L_h = 1.07 \text{mm}$ $L_p = 2 \sim 2.35 \text{mm}$ $\frac{L_p}{F_p} = 0.8 \sim 1.94$
				<p>Uncertainties</p> j – 80.5% data within 10% f – 85.3% data within 10%

Table 6.1 Heat Exchanger Correlations: Round Tube

Fin type	Surface condition	Author (year)	Correlations	Range of parameters / Comments
Louver	Frosted		N/A	
Slit	Dry	Wang <i>et al.</i> (1999b)	<p>j – factor correlation</p> $j = 1.6409 \text{Re}_{D_c}^{J_1} \left(\frac{S_p}{S_h} \right)^{1.16} \left(\frac{P_t}{P_l} \right)^{1.37} \left(\frac{F_p}{D_c} \right)^{J_2} N^{J_3}$ <p>where,</p> $J_1 = -0.674 + \frac{0.1316N}{\ln(\text{Re}_{D_c})} - 0.3769 \frac{F_p}{D_c} - \frac{1.8857N}{\text{Re}_{D_c}}$ $J_2 = -0.0178 + \frac{0.996N}{\ln(\text{Re}_{D_c})} + \frac{26.7N}{\text{Re}_{D_c}}$ $J_3 = 1.865 + \frac{1244.03}{\text{Re}_{D_c}} \frac{F_p}{D_c} - \frac{14.37}{\ln(\text{Re}_{D_c})}$ <p>S_p : Slit pitch S_h : Slit height</p> <p>f – factor correlation</p> $f = 0.3929 \text{Re}_{D_c}^{-3.585 + 0.8846 \frac{F_p}{D_c} + 2.677 \frac{P_t}{P_l}} N^{-0.009 \ln(\text{Re}_{D_c})} \times \left(\frac{S_p}{S_h} \right)^{-2.48} \left(\frac{F_p}{D_c} \right)^{-1.5706 \frac{157.06}{\text{Re}_{D_c}}}$	<p>Parameters</p> $D_c = 10.34 \text{mm}$ $F_p = 1.21 \sim 2.48 \text{mm}$ $P_t = 25.4 \text{mm}$ $P_l = 22 \text{mm}$ $\delta_f = 0.12 \text{mm}$ $S_p = 2.2 \text{mm}$ $S_h = 0.99 \text{mm}$ $N = 1 \sim 6$ (staggered) $\text{Re}_{D_c} = 400 \sim 7000$ <p>Uncertainties j – 83.1% data within 10% f – 92.8% data within 10%</p>

Table 6.1 Heat Exchanger Correlations: Round Tube

Fin type	Surface condition	Author (year)	Correlations	Range of parameters / Comments
Slit	Dry	Kim & Jacobi (2000)	<p>j – factor correlation</p> $j_{uncoated} = 0.2476(\text{Re}_{Dc})^{-0.209} \left(\frac{F_p}{D_c}\right)^{0.4325} \left(\frac{P_t N}{D_c}\right)^{-0.3792}$ $j_{coated} = 0.4313(\text{Re}_{Dc})^{-0.1329} \left(\frac{F_p}{D_c}\right)^{1.001} \left(\frac{P_t N}{D_c}\right)^{-0.4967}$ <p>f – factor correlation</p> $f_{uncoated} = 1.024(\text{Re}_{Dc})^{-0.5123} \left(\frac{F_p}{D_c}\right)^{-0.7315} \left(\frac{P_t N}{D_c}\right)^{0.1666}$ $f_{coated} = 3.826(\text{Re}_{Dc})^{-0.5959} \left(\frac{F_p}{D_c}\right)^{-0.2392} \left(\frac{P_t N}{D_c}\right)^{0.04879}$	<p>Parameters</p> $F_p = 1.3 \sim 1.7\text{mm}$ $D_o = 7.264\text{mm}$ $N = 2 \sim 3$ (staggered) $P_t = 21.65\text{mm}$ $P_l = 12.7\text{mm}$ $\delta_f = 0.076\text{mm}$ $\text{Re}_{Dc} = 550 \sim 2000$ <p>Uncertainties</p> $j_{uncoated}$ – 88% data in 15% j_{coated} – 87% data in 15% $f_{uncoated}$ – 82% data in 20% f_{coated} – 92% data in 10%

Table 6.1 Heat Exchanger Correlations: Round Tube

Fin type	Surface condition	Author (year)	Correlations	Range of parameters / Comments
Slit	Wet	Kim & Jacobi (2000)	<p>j – factor correlation</p> $j_{uncoated} = 0.3647(\text{Re}_{Dc})^{-0.1457} \left(\frac{F_p}{D_c}\right)^{1.21} \left(\frac{P_l N}{D_c}\right)^{-0.3181}$ $j_{coated} = 0.4559(\text{Re}_{Dc})^{-0.2382} \left(\frac{F_p}{D_c}\right)^{0.7139} \left(\frac{P_l N}{D_c}\right)^{-0.6768}$ <p>f – factor correlation</p> $f_{uncoated} = 1.265(\text{Re}_{Dc})^{-0.2991} \left(\frac{F_p}{D_c}\right)^{-0.2918} \left(\frac{P_l N}{D_c}\right)^{-0.1985}$ $f_{coated} = 0.502(\text{Re}_{Dc})^{-0.2593} \left(\frac{F_p}{D_c}\right)^{0.1516} \left(\frac{P_l N}{D_c}\right)^{0.5522}$	<p>Parameters</p> $F_p = 1.3 \sim 1.7\text{mm}$ $D_o = 7.264\text{mm}$ $N = 2 \sim 3$ (staggered) $P_t = 21.65\text{mm}$ $P_l = 12.7\text{mm}$ $\delta_f = 0.076\text{mm}$ $\text{Re}_{Dc} = 550 \sim 2000$ <p>Uncertainties</p> $j_{uncoated}$ – 90% data in 15% j_{coated} – 95% data in 15% $f_{uncoated}$ – 92% data in 20% f_{coated} – 94% data in 20% <p>Contact angles</p> ‘uncoated’: $\theta_A = 87.5^\circ$ $\theta_R = 40.4^\circ$ ‘coated’: $\theta_A = 9.6^\circ$ $\theta_R = 4.3^\circ$
Slit	Frosted		N/A	

Table 6.1 Heat Exchanger Correlations: Round Tube

Fin type	Surface condition	Author (year)	Correlations	Range of parameters / Comments
Wavy	Dry	Wang <i>et al.</i> (1997b)	j & f – factor correlations $j = \frac{1.201}{[\ln(\text{Re}_{Dc}^\sigma)]^{2.921}}$ $f = \frac{16.67}{[\ln(\text{Re}_{Dc})]^{2.64}} \left(\frac{A_{tot}}{A_{tube}} \right)^{-0.096} N^{0.098}$ where, $\sigma = \frac{A_{min}}{A_{face}}$	* Herringbone wavy fin Parameters $F_p = 1.69 \sim 3.53mm$ $D_c = 10.3mm$ $P_t = 25.4mm$ $P_l = 19.05mm$ $N = 1 \sim 4$ (staggered) $\delta_f = 0.12mm$ $\text{Re}_{Dc} = 350 \sim 7000$ Uncertainties j – 94% data within 10% f – 95% data within 15%

Table 6.1 Heat Exchanger Correlations: Round Tube

Fin type	Surface condition	Author (year)	Correlations	Range of parameters / Comments
Wavy	Wet	Wang <i>et al.</i> (1999c)	<p><u>j – factor correlation</u></p> $j = 0.472293 \text{Re}_{D_c}^{J1} \left(\frac{P_t}{P_l}\right)^{J2} \left(\frac{P_d}{X_f}\right)^{J3} \left(\frac{P_d}{F_p - \delta_f}\right)^{J4} N^{-0.4933}$ <p>where,</p> $J1 = -0.5836 + 0.2371 \left(\frac{F_p - \delta_f}{D_c}\right)^{0.55} N^{0.34} \left(\frac{P_t}{P_l}\right)^{1.2}$ $J2 = 1.1873 - 3.0219 \left(\frac{F_p - \delta_f}{D_c}\right)^{1.5} \left(\frac{P_d}{X_f}\right)^{0.9} [\ln(\text{Re}_{D_c})]^{1.22}$ $J3 = 0.006672 \left(\frac{P_t}{P_l}\right) N^{1.96}$ $J4 = -0.1157 \left(\frac{F_p - \delta_f}{D_c}\right)^{0.9} \ln\left(\frac{50}{\text{Re}_{D_c}}\right)$ <p>P_d : wave height X_f : half projected wave length</p>	<p>* Herringbone wavy fin</p> <p>Parameters $F_p = 1.7 \sim 3.1\text{mm}$ $\delta_f = 0.12\text{mm}$ $D_c = 8.62 \sim 10.38\text{mm}$ $P_t = 25.4\text{mm}$ $P_l = 19 \sim 22\text{mm}$ $P_d = 1.18 \sim 1.58\text{mm}$ $N = 1 \sim 6$ (staggered) $\text{Re}_{D_c} = 300 \sim 3500$</p> <p>Uncertainties j – 93.8% data within 15% f – 84.1% data within 15%</p>

Table 6.1 Heat Exchanger Correlations: Round Tube

Fin type	Surface condition	Author (year)	Correlations	Range of parameters / Comments
Wavy	Wet	Wang <i>et al.</i> (1999c)	<p><u>f – factor correlation</u></p> $f = 0.149001 \text{Re}_{D_c}^{F1} \left(\frac{P_t}{P_l}\right)^{F2} N^{F3} \ln\left(3.1 - \frac{P_d}{X_f}\right)^{F4} \left(\frac{F_p}{D_c}\right)^{F5} \left(\frac{2\Gamma}{\mu_f}\right)^{0.0769}$ <p>where,</p> $F1 = -0.067 + \left(\frac{P_d}{F_p - \delta_f}\right) \left(\frac{1.35}{\ln(\text{Re}_{D_c})}\right) - 0.15 \left(\frac{N}{\ln(\text{Re}_{D_c})}\right) + 0.0153 \left(\frac{F_p - \delta_f}{D_c}\right)$ $F2 = 2.981 - 0.082 \ln(\text{Re}_{D_c}) + \frac{0.127N}{4.605 - \ln(\text{Re}_{D_c})}$ $F3 = 0.53 - 0.0491 \ln(\text{Re}_{D_c})$ $F4 = 11.91 \left(\frac{N}{\ln(\text{Re}_{D_c})}\right)^{0.7}$ $F5 = -1.32 + 0.287 \ln(\text{Re}_{D_c})$ <p> $\Gamma = \frac{\dot{m}}{WN}$: condensate flow rate per unit width per tube row μ_f : dynamic viscosity of water </p>	
Wavy	Frosted		N/A	

Table 6.1 Heat Exchanger Correlations: Flat Tube

Fin type	Surface condition	Author (year)	Correlations	Range of parameters / Comments
Plain	Dry		N/A	
Plain	Wet		N/A	
Plain	Frosted		N/A	
Louver	Dry	Chang & Wang (1997)	<p><u>j</u> – factor correlation</p> $j = \text{Re}_{L_p}^{-0.49} \left(\frac{\theta}{90} \right)^{0.27} \left(\frac{F_p}{L_p} \right)^{-0.14} \left(\frac{F_l}{L_p} \right)^{-0.29} \left(\frac{T_d}{L_p} \right)^{-0.23}$ $\times \left(\frac{L_l}{L_p} \right)^{0.68} \left(\frac{T_p}{L_p} \right)^{-0.28} \left(\frac{\delta_f}{L_p} \right)^{-0.05}$ <p>where, F_l : fin length, L_p : louver pitch, L_l : louver length T_d : tube depth, T_p : tube pitch, θ : louver angle</p>	<p>* Based on 91-coil data from other reports</p> <p>Parameters $\text{Re}_{L_p} = 100 \sim 3000$ $L_p = 0.5 \sim 3\text{mm}$ $L_l = 0.94 \sim 18.5\text{mm}$ $\theta = 8.43 \sim 35^\circ$ $F_p = 0.51 \sim 3.33\text{mm}$ $T_d = 15.6 \sim 50\text{mm}$ $F_l = 6 \sim 20\text{mm}$ $\delta_f = 0.04 \sim 0.16\text{mm}$ $T_p = 7.51 \sim 25\text{mm}$ $D_h = 0.824 \sim 4.94\text{mm}$</p> <p>Uncertainty j – 89.3% corrugated louver data within 15%</p>

Table 6.1 Heat Exchanger Correlations: Flat Tube

Fin type	Surface condition	Author (year)	Correlations	Range of parameters / Comments
Louver	Dry	Chang <i>et al.</i> (2000)	<p><u>f – factor correlation</u></p> $f = f1 * f2 * f3$ <p>where, if $Re_{Lp} < 150$,</p> $f1 = 14.39 Re_{Lp}^{\left(-0.805 \frac{F_p}{F_l}\right)} \left(\ln \left(1.0 + \left(\frac{F_p}{L_p} \right) \right) \right)^{3.04}$ $f2 = \left(\ln \left(\left(\frac{F_l}{F_p} \right)^{0.48} + 0.9 \right) \right)^{-1.435} \left(\frac{D_h}{L_p} \right)^{-3.01} \left(\ln(0.5 Re_{Lp}) \right)^{-3.01}$ $f3 = \left(\frac{F_p}{L_l} \right)^{-0.308} \left(\frac{F_d}{L_l} \right)^{-0.308} \left(e^{-0.1167 \frac{T_p}{D_m}} \theta \right)^{0.35}$ <p>if $150 < Re_{Lp} < 5000$,</p> $f1 = 4.97 Re_{Lp}^{\left(0.6049 - \frac{1.064}{\theta^{0.2}}\right)} \left(\ln \left(\left(\frac{\delta_f}{F_p} \right)^{0.5} + 0.9 \right) \right)^{-0.527}$ $f2 = \left(\left(\frac{D_h}{L_p} \right) \ln(0.3 Re_{Lp}) \right)^{-2.966} \left(\frac{F_p}{L_l} \right)^{-0.7931 \left(\frac{T_p}{T_h} \right)}$ $f3 = \left(\frac{T_p}{D_m} \right)^{-0.0446} \ln \left(1.2 + \left(\frac{L_p}{F_p} \right)^{1.4} \right)^{-3.553} \theta^{-0.477}$ <p>$T_h = T_p - D_m$; D_m: major tube diameter</p>	<p>* Same databank and parameters as Wang & Chang (1997)</p> <p>Uncertainty f – 83.14% data within 15%</p>

Table 6.1 Heat Exchanger Correlations: Flat Tube

Fin type	Surface condition	Author (year)	Correlations	Range of parameters / Comments
Louver	Wet		N/A	
Louver	Frosted		N/A	
Slit	Dry	Manglik & Bergles (1995)	<p><u>j & f – factor correlation</u></p> $j = 0.6522 \text{Re}_{Dh}^{-0.5403} \alpha^{-0.1541} \delta^{0.1499} \gamma^{-0.0678}$ $\times \left(1 + 5.269 \cdot 10^{-5} \text{Re}_{Dh}^{1.340} \alpha^{0.504} \delta^{0.456} \gamma^{-1.055}\right)^{0.1}$ $f = 9.6243 \text{Re}_{Dh}^{-0.7422} \alpha^{-0.1856} \delta^{0.3053} \gamma^{-0.2659}$ $\times \left(1 + 7.669 \cdot 10^{-8} \text{Re}_{Dh}^{4.429} \alpha^{0.920} \delta^{3.767} \gamma^{0.236}\right)^{0.1}$ $\alpha = \frac{s}{h}, \quad \delta = \frac{t}{l}, \quad \gamma = \frac{t}{s}$ <p>where, s: lateral fin spacing t: fin thickness l: fin length</p>	* Rectangular offset strip fin Parameters $\text{Re}_{Dh} = 300 \sim 5000$ $D_h = 1.209 \sim 3.414 \text{mm}$ $\alpha = 0.134 \sim 0.997$ $\delta = 0.012 \sim 0.048$ $\gamma = 0.041 \sim 0.121$
Slit	Wet		N/A	
Slit	Frosted		N/A	
Wavy	Dry		N/A	
Wavy	Wet		N/A	
Wavy	Frosted		N/A	

Table 6.1 Heat Exchanger Correlations: Flat Tube

Fin type	Surface condition	Author (year)	Correlations	Range of parameters / Comments																																																								
Louver	Dry	Park and Jacobi (2009a)	<p><u><i>j</i> and <i>f</i> – correlations</u></p> $j_{\text{cor}} = C_1 j_{\text{Re}} j_{\text{low}} j_{\text{louver}} \theta^{C_2} N_{\text{LB}}^{C_3} \left(\frac{F_1}{L_p}\right)^{C_4} \left(\frac{T_d}{F_p}\right)^{C_5} \left(\frac{L_1}{F_1}\right)^{C_6} \times \left(\frac{F_1}{T_p}\right)^{C_7} \left(1 - \frac{\delta_f}{L_p}\right)^{C_8} \left(\frac{L_p}{F_p}\right)^{C_9}$ $j_{\text{Re}} = Re_{Lp} \left[C_{10} + C_{11} \cosh\left(\frac{F_p}{L_p} - 1\right) \right]$ $j_{\text{low}} = 1 - \sin\left(\frac{L_p}{F_p} \cdot \theta\right) \left[\cosh\left(C_{12} Re_{Lp} - C_{13} \frac{T_d}{N_{\text{LB}} F_p} \right) \right]^{-1}$ $j_{\text{louver}} = 1 - C_{14} \tan(\theta) \left(\frac{T_d}{N_{\text{LB}} F_p}\right) \cos\left[2\pi \left(\frac{F_p}{L_p \tan(\theta)} - 1.8\right) \right]$ $f_{\text{cor}} = D_1 f_{\text{Re}} N_{\text{LB}}^{D_2} \left(\frac{F_p}{L_p}\right)^{D_3} \sin(\theta + D_4) \left(1 - \frac{F_1}{T_p}\right)^{D_5} \left(\frac{L_1}{F_1}\right)^{D_6} \left(\frac{\delta_f}{L_p}\right)^{D_7} \left(\frac{F_1}{F_p}\right)^{D_8}$ $f_{\text{Re}} = \left(Re_{Lp} \cdot \frac{F_p}{L_p} \right)^{D_9} + D_{10} Re_{Lp} \left[D_{11} \left(\frac{\delta_f}{F_p}\right) \right]$	<p>* 1030 heat transfer and 1270 pressure drop data, 126 samples</p> <p>Parameters $Re_{Lp} = 27 \sim 4132$ $L_p = 0.5 \sim 3\text{mm}$ $L_t = 0.94 \sim 18.5\text{mm}$ $\theta = 8.43 \sim 35^\circ$ $F_p = 0.51 \sim 5.08\text{mm}$ $T_d = 15.6 \sim 57.4\text{mm}$ $F_l = 2.84 \sim 20\text{mm}$ $\delta_f = 0.0254 \sim 0.16\text{mm}$ $T_p = 3.76 \sim 25\text{mm}$ N_{LB} up to 4</p> <p>Uncertainty <i>j</i> – RMS 11.5% <i>f</i> – RMS 16.1%</p>																																																								
			<table border="1"> <tbody> <tr><td>C_1</td><td>0.8723</td><td>C_8</td><td>2.624</td><td>D_1</td><td>3.689</td><td>D_7</td><td>-0.6474</td></tr> <tr><td>C_2</td><td>0.2190</td><td>C_9</td><td>0.3005</td><td>D_2</td><td>-0.2563</td><td>D_8</td><td>0.7986</td></tr> <tr><td>C_3</td><td>-0.0881</td><td>C_{10}</td><td>-0.4578</td><td>D_3</td><td>0.9041</td><td>D_9</td><td>-0.8454</td></tr> <tr><td>C_4</td><td>0.1491</td><td>C_{11}</td><td>-0.008737</td><td>D_4</td><td>0.2004</td><td>D_{10}</td><td>0.001298</td></tr> <tr><td>C_5</td><td>-0.2585</td><td>C_{12}</td><td>0.04897</td><td>D_5</td><td>0.7330</td><td>D_{11}</td><td>1.259</td></tr> <tr><td>C_6</td><td>0.5400</td><td>C_{13}</td><td>0.1417</td><td>D_6</td><td>0.6481</td><td></td><td></td></tr> <tr><td>C_7</td><td>-0.9023</td><td>C_{14}</td><td>-0.0065</td><td></td><td></td><td></td><td></td></tr> </tbody> </table>	C_1	0.8723	C_8	2.624	D_1	3.689	D_7	-0.6474	C_2	0.2190	C_9	0.3005	D_2	-0.2563	D_8	0.7986	C_3	-0.0881	C_{10}	-0.4578	D_3	0.9041	D_9	-0.8454	C_4	0.1491	C_{11}	-0.008737	D_4	0.2004	D_{10}	0.001298	C_5	-0.2585	C_{12}	0.04897	D_5	0.7330	D_{11}	1.259	C_6	0.5400	C_{13}	0.1417	D_6	0.6481			C_7	-0.9023	C_{14}	-0.0065					
C_1	0.8723	C_8	2.624	D_1	3.689	D_7	-0.6474																																																					
C_2	0.2190	C_9	0.3005	D_2	-0.2563	D_8	0.7986																																																					
C_3	-0.0881	C_{10}	-0.4578	D_3	0.9041	D_9	-0.8454																																																					
C_4	0.1491	C_{11}	-0.008737	D_4	0.2004	D_{10}	0.001298																																																					
C_5	-0.2585	C_{12}	0.04897	D_5	0.7330	D_{11}	1.259																																																					
C_6	0.5400	C_{13}	0.1417	D_6	0.6481																																																							
C_7	-0.9023	C_{14}	-0.0065																																																									

Table 6.1 Heat Exchanger Correlations: Flat Tube

Fin type	Surface condition	Author (year)	Correlations	Range of parameters / Comments																												
Louver	Wet	Park and Jacobi (2009b)	<p><u><i>j</i> and <i>f</i> – correlation</u></p> $j_{\text{cor}} = a_1 Re_{Lp}^{a_2} \left(\frac{L_p}{F_p}\right)^{a_3} (\sin(\alpha))^{a_4} \left(\frac{L_l}{F_l}\right)^{a_5} \left(\frac{F_d}{F_p}\right)^{a_6} \left(\frac{F_l}{T_p}\right)^{a_7}$ $f_{\text{cor}} = b_1 + b_2 Re_{Lp}^{b_3} \left(\frac{L_p}{F_p}\right)^{b_4} (\sin(\alpha))^{b_5} \left(\frac{F_l}{T_p}\right)^{b_6}$ <table border="1" style="margin-left: auto; margin-right: auto;"> <tr> <td>a_1</td> <td>0.4260</td> <td>b_1</td> <td>0.07400</td> </tr> <tr> <td>a_2</td> <td>-0.3149</td> <td>b_2</td> <td>152.7</td> </tr> <tr> <td>a_3</td> <td>0.6705</td> <td>b_3</td> <td>-1.116</td> </tr> <tr> <td>a_4</td> <td>0.3489</td> <td>b_4</td> <td>2.242</td> </tr> <tr> <td>a_5</td> <td>0.5123</td> <td>b_5</td> <td>0.9680</td> </tr> <tr> <td>a_6</td> <td>-0.2698</td> <td>b_6</td> <td>1.716</td> </tr> <tr> <td>a_7</td> <td>-0.2845</td> <td></td> <td></td> </tr> </table>	a_1	0.4260	b_1	0.07400	a_2	-0.3149	b_2	152.7	a_3	0.6705	b_3	-1.116	a_4	0.3489	b_4	2.242	a_5	0.5123	b_5	0.9680	a_6	-0.2698	b_6	1.716	a_7	-0.2845			<p>* 166 heat transfer and 196 pressure drop data, 47 samples</p> <p>Parameters $Re_{Lp} = 50 \sim 1400$ $L_p = 0.95 \sim 2.66\text{mm}$ $L_l = 6.15 \sim 11.15\text{mm}$ $\theta = 15 \sim 42^\circ$ $F_p = 1.0 \sim 5.08\text{mm}$ $T_d = 15.6 \sim 57.4\text{mm}$ $F_l = 7.93 \sim 12.43\text{mm}$ $\delta_f = 0.08 \sim 0.15\text{mm}$ $T_p = 9.7 \sim 15.7\text{mm}$ N_{LB} up to 4</p> <p>Uncertainty <i>j</i> – RMS 22.7% <i>f</i> – RMS 29.1%</p>
a_1	0.4260	b_1	0.07400																													
a_2	-0.3149	b_2	152.7																													
a_3	0.6705	b_3	-1.116																													
a_4	0.3489	b_4	2.242																													
a_5	0.5123	b_5	0.9680																													
a_6	-0.2698	b_6	1.716																													
a_7	-0.2845																															
Louver	Wet		N/A																													
Louver	Frosted		N/A																													

Table 6.1 Heat Exchanger Correlations: Flat Tube

Fin type	Surface condition	Author (year)	Correlations	Range of parameters / Comments
Slit	Dry	Manglik & Bergles (1995)	<u>j & f – factor correlation</u> $j = 0.6522 \text{Re}_{Dh}^{-0.5403} \alpha^{-0.1541} \delta^{0.1499} \gamma^{-0.0678}$ $\times \left(1 + 5.269 \cdot 10^{-5} \text{Re}_{Dh}^{1.340} \alpha^{0.504} \delta^{0.456} \gamma^{-1.055}\right)^{0.1}$ $f = 9.6243 \text{Re}_{Dh}^{-0.7422} \alpha^{-0.1856} \delta^{0.3053} \gamma^{-0.2659}$ $\times \left(1 + 7.669 \cdot 10^{-8} \text{Re}_{Dh}^{4.429} \alpha^{0.920} \delta^{3.767} \gamma^{0.236}\right)^{0.1}$ $\alpha = \frac{s}{h}, \quad \delta = \frac{t}{l}, \quad \gamma = \frac{t}{s}$ <p>where, s: lateral fin spacing t: fin thickness l: fin length</p>	* Rectangular offset strip fin Parameters $\text{Re}_{Dh} = 300 \sim 5000$ $D_h = 1.209 \sim 3.414 \text{mm}$ $\alpha = 0.134 \sim 0.997$ $\delta = 0.012 \sim 0.048$ $\gamma = 0.041 \sim 0.121$
Slit	Wet		N/A	
Slit	Frosted		N/A	
Wavy	Dry		N/A	
Wavy	Wet		N/A	
Wavy	Frosted		N/A	

Example 6.1:

Consider a heat exchanger that is comprised of one row of four, annularly finned tubes, as shown in Figure 6.3 Annular-fin-tube heat exchanger. Hot air flows upward over the outside surfaces of the tubes, and water flows through the insides of the tubes, as a single pass (into the page). The inside and outside radii of the tube are $r_{ii}=3.5$ and $r_i=5.0$ mm, respectively, and the tubes have a length of $L_c=0.5$ m and a thermal conductivity of $k_f=180$ W/(mK). The outer fin radius is $r_o=20$ mm, its thickness is $\delta=0.3$ mm, the fin pitch is $P_f=50$ fins/m. Water enters at $T_{ci}=20$ C and flows at a total mass flow rate of $m_c=0.15$ kg/s. The air flows with a velocity of $V_{fr}=3$ m/s at the frontal face of the heat exchanger and enters with a temperature of $T_{hi}=800$ C.

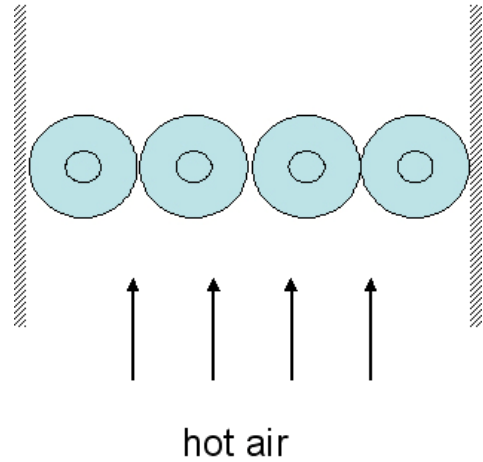


Figure 6.3 Annular-fin-tube heat exchanger

For this heat exchanger operating under these steady-state conditions, find the total rate of heat transfer using both the *LMTD* and an ε - N_{TU} approaches.

Solution by LMTD: In this method, the rate equation and energy balance on the water and air streams takes the following form:

$$Q = UA \cdot F \cdot \left[\frac{(T_{hi} - T_{co}) - (T_{ho} - T_{ci})}{\log \left\{ \frac{T_{hi} - T_{co}}{T_{ho} - T_{ci}} \right\}} \right] \quad Q = m_c c_c (T_{co} - T_{ci}) \quad Q = \rho_{ai} A_{fr} V_{fr} c_a (T_{ai} - T_{ao})$$

For a prescribed geometry and inlet conditions, with known properties, assuming UA can be determined, these three equations still have four unknowns, T_{ho} , T_{co} , Q , and F . The cross-flow correction factor, F , depends on inlet and outlet temperatures. Thus, solving the problem by *LMTD* will require iteration. A good practice is to start by assuming $F=1$, then solve the three equations for T_{ho} , T_{co} , and Q , find a new value of F and iterate until the answers are changing by an acceptable tolerance. In this spirit, the equation set needed for the *LMTD* approach is provided in Table 6.2. In the table, the unknown variables introduced by each equation are listed. All properties are assumed known, realizing that their evaluation might also require iteration due to their temperature dependence. Solving the set of 22 equations in the table yields values for the 22 listed unknowns. It is found that $Q=2430$ W, $T_{co}=23.9$ C, and $T_{ho}=773.2$ C. Using these temperatures, it is found graphically that $F \approx 1$ (from Incropera *et al.*, 2007); thus further iteration was not pursued. While it is found that $Re_c=6810$, which suggests a more sophisticated correlation for h_c might be required (e.g. that due to Gnielinski), it is also found that $R_{Ti}=3.1(10^{-1})$ K/W and $R_{Tc}=4.6(10^{-3})$ K/W; thus, the heat exchanger is air-side limited and refining the tube-side modeling is not necessary.

Table 6.2 Equation Set for an LMTD Solution

Equation	Unknowns
$Re_c = 2(m_c / 4) / (\pi r_{ii} \mu_c)$	Re_c
$h_c = (0.023 Re_c^{0.8} Pr_c^{0.4}) k_c / (2r_{ii})$ (based on Dittus-Boelter)	h_c
$R_{Tc} = 1 / (h_c 8\pi r_{ii} L_c)$	R_{Tc}
$A_{fr} = 4(2r_o) L_c$	A_{fr}
$N_{fin} = 4(P_f L_c)$	N_{fin}
$A_{fin} = N_{fin} [2\pi(r_o^2 - r_i^2) + 2\pi r_o \delta]$	A_{fin}
$A_{Th} = 4(2\pi r_i L_c) - N_{fin}(2\pi r_i \delta) + A_{fin}$	A_{Th}
$A_{min} = A_{fr} - 4(2r_i L) - N_{fin} 2(r_o - r_i) \delta$	A_{min}
$D_h = 4A_{min}(2r_o) / A_{Th}$	D_h
$m_h = \rho_{h,i} V_{fr} A_{fr}$	m_h
$Re_h = m_h D_h / (A_{min} \mu_h)$	Re_h
$j_h = 0.0265 Re_h^{-0.22}$ (Kearney and Jacobi, 1995)	j_h
$h_h = j_h m_h c_h / (A_{min} Pr_h^{2/3})$	h_h
$m = \sqrt{r_o^2 2h_h / (k\delta)}$	m
$\eta_f = \frac{2r_i r_o}{m(r_o^2 - r_i^2)} \left[I_1(m) K_1\left(\frac{mr_i}{r_o}\right) - K_1(m) I_1\left(\frac{mr_i}{r_o}\right) \right] \left[I_0\left(\frac{mr_i}{r_o}\right) K_1(m) + I_1(m) K_0\left(\frac{mr_i}{r_o}\right) \right]^{-1}$	η_f
$\eta_o = 1 - A_{fin}(1 - \eta_f) / A_{Th}$	η_o
$R_{Th} = 1 / (h_h \eta_o A_{Th})$	R_{Th}
$R_{Tw} = \ln(r_o / r_i) / (8\pi L_c k_w)$	R_{Tw}
$UA = (R_{Tc} + R_{Tw} + R_{Th})^{-1}$	UA
$Q = m_h c_h (T_{hi} - T_{ho})$	Q, T_{ho}
$Q = m_c c_c (T_{co} - T_{ci})$	T_{co}
$Q = UA \cdot F \cdot \left[(T_{hi} - T_{co}) - (T_{ho} - T_{ci}) \right] / \log \left\{ \frac{T_{hi} - T_{co}}{T_{ho} - T_{ci}} \right\}$ (take $F=1$, iterate)	

Solution by ε - N_{TU} : In this method, the rate equation follows Eq. [6.1.6] and the functional form of the ε - N_{TU} relationship depends on heat exchanger configuration. The equation set for this method is provided in Table 6.3. Note that the methods are identical, except for the way the rate equation is handled. The ε - N_{TU} approach takes care of F through the functional form of the ε - N_{TU} relationship graphical evaluations of F and iteration are not required by this method. The solution obtained with the 24 equations in Table 6.3 is the same as that obtained by *LMTD*—as it should be.

Table 6.3 Equation Set for an εN_{TU} Solution

Equation	Unknowns
$Re_c = 2(m_c / 4) / (\pi r_{ii} \mu_c)$	Re_c
$h_c = (0.023 Re_c^{0.8} Pr_c^{0.4}) k_c / (2r_{ii})$ (based on Dittus-Boelter)	h_c
$R_{Tc} = 1 / (h_c 8\pi r_{ii} L_c)$	R_{Tc}
$A_{fr} = 4(2r_o) L_c$	A_{fr}
$N_{fin} = 4(P_f L_c)$	N_{fin}
$A_{fin} = N_{fin} [2\pi(r_o^2 - r_i^2) + 2\pi r_o \delta]$	A_{fin}
$A_{Th} = 4(2\pi r_i L_c) - N_{fin} (2\pi r_i \delta) + A_{fin}$	A_{Th}
$A_{min} = A_{fr} - 4(2r_i L) - N_{fin} 2(r_o - r_i) \delta$	A_{min}
$D_h = 4A_{min} (2r_o) / A_{Th}$	D_h
$m_h = \rho_{h,i} V_{fr} A_{fr}$	m_h
$Re_h = m_h D_h / (A_{min} \mu_h)$	Re_h
$j_h = 0.0265 Re_h^{-0.22}$ (Kearney and Jacobi, 1995)	j_h
$h_h = j_h m_h c_h / (A_{min} Pr_h^{2/3})$	h_h
$m = \sqrt{r_o^2 2h_h / (k\delta)}$	m
$\eta_f = \frac{2r_i r_o}{m(r_o^2 - r_i^2)} \left[I_1(m) K_1\left(\frac{mr_i}{r_o}\right) - K_1(m) I_1\left(\frac{mr_i}{r_o}\right) \right] \left[I_0\left(\frac{mr_i}{r_o}\right) K_1(m) + I_1(m) K_0\left(\frac{mr_i}{r_o}\right) \right]^{-1}$	η_f
$\eta_o = 1 - A_{fin} (1 - \eta_f) / A_{Th}$	η_o
$R_{Th} = 1 / (h_h \eta_o A_{Th})$	R_{Th}
$R_{Tw} = \ln(r_o / r_i) / (8\pi L_c k_w)$	R_{Tw}
$UA = (R_{Tc} + R_{Tw} + R_{Th})^{-1}$	UA
$Q = m_h c_h (T_{hi} - T_{ho})$	Q, T_{ho}
$Q = m_c c_c (T_{co} - T_{ci})$	T_{co}
$Q = \varepsilon (m_h c_h) (T_{hi} - T_{ci})$ (hot stream is minimum mc)	ε
$N_{tu} = UA / (m_h c_h)$	N_{TU}
$\varepsilon = \frac{m_c c_c}{m_h c_h} \left[1 - \exp \left\{ -\frac{m_h c_h}{m_c c_c} (1 - e^{-N_{TU}}) \right\} \right]$	

6.9 Nomenclature

A, B, C, D	constants
A_{fin}	heat transfer area associated with fins
A_{fr}	frontal area, <i>i.e.</i> , cross-sectional flow area just upstream of inlet face
A_{min}	minimum cross-sectional flow area, corresponding to maximum velocity
A_T	total heat transfer area
C_1, C_2	constants
C_r	heat rate capacity ratio, $(Wc)_{min}/(Wc)_{max}$
c	specific heat
Δp	pressure drop
D_c	outer diameter of a tube collar, or outside tube diameter if no collar
D_h	air-side hydraulic, $D_h=4A_{min}L/A_T$
D_m	minor diameter of a flat tube (see Fig. 6.2)
F	flow-arrangement correction factor (see Eq. 6.1.5)
F_l	fin length (see Fig. 6.2)
F_p	fin spacing (see Fig. 6.2)
f	Fanning friction factor (see Eq. 6.1.13)
G	mass flux at minimum flow cross-sectional area, $G=W/A_{min}$
h	heat transfer coefficient, or strip height in an offset-strip fin (see Fig. 6.2)
Δi_{lmcf}	log-mean enthalpy difference, counter-flow (see Eq. 6.1.11)
i	enthalpy
j	Colburn j factor, $j=Nu/(RePr^{1/3})$
K_c	pressure-drop coefficient for contraction (see Eq. 6.1.13)
K_e	pressure-drop coefficient for expansion (see Eq. 6.1.13)
k	thermal conductivity
l	the length of a strip in an offset-strip fin (see Fig. 6.2)
L	air-side flow depth, the distance from inlet to outlet face
L_p	louver spacing (see Fig. 6.2)
L_l	louver length (see Fig. 6.2)
N	number of tube rows in the air-flow direction
N_{tu}	number of thermal units, $N_{tu}=UA/(Wc)_{min}$
Nu	Nusselt number, $Nu=hD_h/k$
P	fan power
P_l	center-to-center tube spacing in air flow direction (see Fig. 6.2)
P_d	wave amplitude of a wavy fin (see Fig. 6.2)
P_t	center-to-center tube spacing transverse to air flow direction (see Fig. 6.2)
Pr	Prandtl number, $Pr=c\mu/k$
Q	heat transfer rate
Q_{max}	maximum possible heat transfer $Q_{max}=(Wc)_{min}\Delta T_{max}$
R	heat transfer resistance
Re	Reynolds number, $Re=WD_h/(A_{min}\bar{\mu})$, subscript can indicate different scale
S	distance between strips in an offset-strip fin (see Fig. 6.2)
ΔT_{lmcf}	log-mean temperature difference, counter-flow (see Eq. 6.1.5)
ΔT_{max}	hot fluid entering temperature minus cold fluid entering temperature
T	temperature
T_d	major diameter of a flat tube (see Fig. 6.2)

T_p	tube spacing (see Fig. 6.2)
t	strip thickness in an offset-strip fin (see Fig. 6.2)
UA	overall heat transfer conductance
W	mass flow rate
X_f	half the wavelength of a wavy fin (see Fig. 6.2)

Greek Symbols

α	geometric parameter in an offset-strip fin (see Fig. 6.2), $\alpha=s/h$
δ	geometric parameter in an offset-strip fin (see Fig. 6.2), $\delta=t/l$
δ_f	fin thickness (see Fig. 6.2)
ε	heat exchanger effectiveness, $\varepsilon=Q/Q_{max}$
η_f	fin efficiency, geometry dependent (see Incropera et al., 2007)
η_o	overall surface efficiency, $\eta_o=1-(A_{fin}/A_T)(1-\eta_f)$
γ	geometric parameter in an offset-strip fin (see Fig. 6.2), $\gamma=t/s$
μ	dynamic viscosity
ρ	density
σ	contraction ratio, A_{min}/A_f

Other subscripts

a	air or air side
$contact$	associated with thermal resistance due to contact (see Eq. 6.1.7)
f	fin
$foul$	associated with thermal resistance due to fouling (see Eq. 6.1.7)
i	in
L_p	based on louver spacing
max	maximum
min	minimum
o	out, or overall
r	ratio
T	tube
t	tube side
$wall$	associated with thermal resistance due to conduction (see Eq. 6.1.7)

overbar indicates an average

6.10 REFERENCES

- Abu Madi, M., Johns, R.A. and Heikal, M.R. (1998).** Performance Characteristics Correlation for Round Tube and Plate Finned Heat Exchangers, *Int. J. Refrigeration*, Vol. 21(7), pp. 507-517.
- Achaichia, A. and Cowell, T.A. (1988).** Heat Transfer and Pressure Drop Characteristics of Flat Tube and Louvered Plate Fin Surfaces, *Exp. Thermal Fluid Sci.*, Vol. 1(2), pp. 147-157.
- Chang, Y.J. and Wang, C.C. (1997).** A Generalized Heat Transfer Correlation for Louver Fin Geometry, *Int. J. Heat Mass Transfer*, Vol. 40(3), pp. 533-544.
- Chang, W.R., Wang, C.C., Tsi, W.C. and Shyu, R.J. (1995).** Air-Side Performance of Louver Fin Heat Exchanger, *4th ASME/JSME Thermal Engineering Joint Conference*, Vol. 4, pp. 467-372.
- Chang, Y.J., Wang, C.C., Shyu, R.J. and Robert, Y.Z. (1995).** Performance Comparison between Automotive Flat Tube Condenser and Round Tube Condenser, *ASME/JSME Thermal Engineering Joint Conference – Proceedings*, Vol. 4, pp. 332-336.
- Chang, Y.J., Hsu, K.C., Lin, Y.T. and Wang, C.C. (2000).** A Generalized Friction Correlation for Louver Fin Geometry, *Int. J. Heat Mass Transfer*, Vol. 43, pp. 2237-2243.
- Davenport, C.J. (1983).** Correlations for Heat Transfer and Flow Friction Characteristics of Louvered Fin, *AIChE Symposium series*, No. 225, pp. 19-27.
- DeJong, N.C. and Jacobi, A.M. (2003a).** Heat Transfer and Pressure Drop for Flow Through Bounded Louvered-Fin Arrays, *Exp. Thermal Fluid Sci.*, 27, 237-250.
- DeJong, N.C. and Jacobi, A.M. (2003b).** Localized Flow and Heat Transfer Interactions in Louvered-Fin Arrays, *Int. J. Heat Mass Transfer*, 46, 443-455.
- Dejong, N.C. and Jacobi, A.M., (1996).** An Experimental Study of Flow and Heat Transfer in Parallel-Plate Arrays: Local, Row-by-row and Surface Average Behavior, *Int. J. Heat Mass Transfer*, Vol. 40(6), pp. 1365-1378.
- DeJong, N.C., Zhang, L.W., Jacobi, A.M., Balachandar, S. and Tafti, D.K. (1998).** A Complementary Experimental and Numerical Study of the Flow and Heat Transfer in Offset Strip-Fin Heat Exchangers, *J. Heat Transfer*, 120, 690-698.
- Du, Y.J. and Wang, C.C. (2000).** An Experimental Study of the Airside Performance of the Superslit Fin-and-Tube Heat Exchangers, *Int. J. Heat Mass Transfer*, Vol. 43, pp. 4475-4482.
- ElSherbini, A. and Jacobi, A.M. (2002).** The Thermal-Hydraulic Impact of Delta-Wing Vortex Generators on the Performance of a Plain-Fin-and-Tube Heat Exchanger, *J. HVAC&R Research*, 8, 357-370.
- ElSherbini, A.I., Jacobi, A.M. and Hrnjak, P.S. (2003).** Experimental Investigation of Thermal Contact Resistance in Plain-Fin-and-Tube Evaporators with Collarless Fins, *Int. J. Refrigeration*, 26:5, 527-536.
- Emery, A.F. and Siegel, B.L. (1990).** Experimental Measurements of the Effects of Frost Formation on Heat Exchanger Performance, *ASME – HTD*, Vol. 139, pp. 1-7.
- Fu, W.L., Wang, C.C., Chang, W.R., and Chang, C.T. (1995).** Effect of Anti-Corrosion Coating on the Thermal Characteristics of Louvered Finned Tube Heat Exchangers under Dehumidifying Conditions, *Advances in Enhanced Heat/Mass Transfer and Energy Efficiency*, HTD-Vol. 320/PID-Vol. 1, ASME, pp. 75-81.
- Gray, D.L. and Webb, R.L. (1986).** Heat Transfer and Friction Correlations for Plate Finned-Tube Heat Exchangers Having Plain Fins, *Proceeding 8th International Journal of Heat Transfer Conference*, Vol. 6, pp. 2745-2750.
- Guillory, J.L. and McQuiston, F.C. (1973).** An Experimental Investigation of Air Dehumidification in a Parallel Plate Exchanger, *ASHRAE Trans.*, Vol. 79, pp. 146-151.
- Incropera, F.P., DeWitt, D.P., Bergman, T.L., and Lavine, A.S., (2007).** *Introduction to Heat Transfer, Fifth Edition*, John Wiley and Sons, New York.

- Jacobi, A.M. and Goldschmidt, V.W. (1990).** Low Reynolds Number Heat and Mass Transfer Measurements of an Overall Counterflow, Baffled, Finned-Tube, Condensing Heat Exchanger, *Int. J. Heat Mass Transfer*, Vol. 33, pp. 755-765.
- Jacobi, A.M., Park, Y., Tafti, D., and Zhang, X. (2001).** An Assessment of the State of the Art, and Potential Design Improvements, for Flat-Tube Heat Exchangers in Air-Conditioning and Refrigeration Applications, Phase I-Final Report, ARTI-21CR/20020-01, University of Illinois, Urbana, IL.
- Jacobi, A.M., Park, Y., Zhong, Y., Michna, G., and Xia, Y. (2005).** High Performance Heat Exchangers for Air-Conditioning and Refrigeration Applications (Non-Circular Tubes), Phase II-Final Report, ARTI-21CR/611-20021, University of Illinois, Urbana, IL.
- Joardar, A. and Jacobi, A.M. (2005).** Impact of Leading Edge Delta-Wing Vortex Generators on the Thermal Performance of a Flat Tube, Louvered-Fin Compact Heat Exchanger, *Int. J. Heat and Mass Transfer*, 48, 1480-1493.
- Joardar, A., and Jacobi, A.M. (2007).** A Numerical Study of Flow and Heat Transfer Enhancement Using an Array of Delta-Winglet Vortex Generators in a Fin-and-Tube Heat Exchanger, *J. Heat Transfer*, 129:9, 1156-1167.
- Joarder, A. and Jacobi, A.M. (2008).** Heat Transfer Enhancement by Winglet-Type-Vortex Generator Arrays in Compact Plain-Fin-and-Tube Heat Exchangers, *Int. J. Refrigeration*, 31:1, 87-97.
- Kaiser, J.M., Jacobi, A.M. (2000).** Condensate retention effects on the air-side heat transfer performance of automotive evaporator coils, CR-32, ACRC, University of Illinois, Urbana, IL, 2000.
- Kays, W.M., and London, A.L. (1955).** *Compact Heat Exchangers*, McGraw-Hill, New York.
- Kays, W.M., and London, A.L. (1984).** *Compact Heat Exchangers*, 3rd edition, McGraw-Hill, New York.
- Kearney, S. P. and A. M. Jacobi, A.M. (1995).** Effects of Gull-Wing Baffles on the Performance of a Single-Row, Annularly Finned Tube Heat Exchanger, *International Journal of HVAC&R Research*, ASHRAE, 1:4, 257-272.
- Kim, G.J. and Jacobi, A.M. (2000).** Condensate Accumulation Effects on the Air-Side Thermal Performance of Slit-Fin Surfaces, CR-26, ACRC, University of Illinois at Urbana-Champaign, IL.
- Kim, N.H., Yun, J.H. and Webb, R.L. (1997).** Heat Transfer and Friction Correlations for Wavy Plate Fin-and-Tube Heat Exchangers, *J. Heat Transfer*, Vol. 119, pp. 560-567.
- Korte, C. and Jacobi, A.M. (2001).** Condensate Retention Effects on the Performance of Plain-Fin-and-Tube Heat Exchangers: Retention Data and Modeling, *J. Heat Transfer*, 123:5, 926-936.
- Liu, L. and Jacobi, A.M. (2009).** Air-Side Surface Wettability Effects on the Performance of Slit-Fin-and-Tube Heat Exchangers Operating under Wet-Surface Conditions, *J. Heat Transfer*, Vol. 131, 051802.
- Manglik, R.M. and Bergles, A.E. (1995).** Heat Transfer and Pressure Drop Correlations for the Rectangular Offset Strip Fin Compact Heat Exchanger, *Experimental Thermal and Fluid Science*, Vol. 10, pp. 171-180.
- McLaughlin, W.J. and Webb, R.L. (2000a).** Condensate Drainage and Retention in Louver Fin Automotive Evaporators, *SAE Technical Paper Series*, No. 2000-01-0575.
- McLaughlin, W.J. and Webb, R.L. (2000b).** Wet Air Side Performance of Louver Fin Automotive Evaporators, *SAE Technical Paper Series*, No. 2000-01-0574.
- McQuiston, F.C. (1978a).** Heat, Mass, and Momentum Transfer Data for Five Plate-Fin-Tube Heat Transfer Surfaces, *ASHRAE Trans.*, Vol. 84, pp. 266-293.
- McQuiston, F.C. (1978b).** Correlation of Heat, Mass, and Momentum Transport Coefficients for Plate-Fin-Tube Heat Transfer Surfaces with Staggered Tubes, *ASHRAE Trans.*, Vol. 109, pp. 294-308
- McQuiston, F.C., and Parker, J.D., (1994).** *Heating, Ventilating, and Air Conditioning: Analysis and Design, Sixth Edition*, John Wiley and Sons, New York.

- Michna, J., Jacobi, A.M., and Burton, R.L. (2007).** An Experimental Study of the Friction Factor and Mass Transfer Performance of an Off-Set Strip Fin Array at Very High Reynolds Numbers, *J. Heat Transfer*, 129:9, 1134-1140.
- Osada, H., Aoki, H., Ohara, T. and Kuroyanagi, I. (1999).** Experimental Analysis for Enhancing Automotive Evaporator Fin Performances, *Compact Heat Exchangers and Enhancement Technology for the Process Industries*, pp. 463-470, Banff, Canada.
- Park, Y. and Jacobi, A.M. (2009a).** Air-side Heat Transfer and Friction Correlations for Flat-tube, Louver-fin Heat Exchangers, *J. Heat Transfer*, 131:2, 021801-1.
- Park, Y. and Jacobi, A.M. (2009b).** The Air-side Thermal-hydraulic Performance of Flat-tube Heat Exchangers with Louvered, Wavy, and Plain Fins Under Dry and Wet Conditions, *J. Heat Transfer*, 131:6, 061801.
- Park, Y. and Jacobi, A.M. (2010).** A Simple Air-Side Data Analysis Method for Partially Wet Flat-Tube Heat Exchangers, *Heat Transfer Engineering*, (sub judice).
- Rich, D.G. (1973).** The Effect of Fin Spacing On the Heat Transfer and Friction Performance of Multi-Row, Smooth Plate Fin-and-Tube Heat Exchangers, *ASHRAE Trans.*, Vol. 79, pp. 137-145.
- Rich, D.G. (1975).** The Effect of the Number of Tube Rows on Heat Transfer Performance of Smooth Plate Fin-and-Tube Heat Exchangers, *ASHRAE Trans.*, Vol. 81, Part 1, pp. 307-317.
- Rush, T.A., Newell, T., and Jacobi, A.M. (1999).** An Experimental Study of Flow and Heat Transfer in Sinusoidal Wavy Passages, *Int. J. Heat and Mass Transfer*, 42, 1541-1553.
- Smotrys, M., Ge, H., Dutton, J.C. and Jacobi, A.M. (2003).** Flow and Heat Transfer Behavior for a Vortex-Enhanced Interrupted Fin, *J. Heat Transfer*, 125:5, 788-794.
- Sommers, A.D., and Jacobi, A.M. (2005).** Air-Side Heat Transfer Enhancement of a Refrigerator Evaporator Using Vortex Generation, *Int. J. Refrigeration*, 28, 1006-1017.
- Sommers, A.D., and Jacobi, A.M. (2006).** An Exact Solution to Steady Heat Conduction in a Two-Dimensional Annulus on a One-Dimensional Fin: Application to Frosted Heat Exchangers with Round Tubes, *J. Heat Transfer*, 128, 397-404.
- Taborek, J., Aoki, T., Ritter, R. B., Palen, J.W., and Knudsen, J.G. (1972).** Fouling – the major unresolved problem in heat transfer, *Chem. Engineering Prog.*, 68(2):59-67.
- Threlkeld, J.L. (1970).** *Thermal Environmental Engineering*, Prentice-Hall Inc., New York, NY.
- Tree, D.R. and Helmer, W.A. (1976).** Experimental Heat and Mass Transfer Data for Condensing Flow in a parallel Plate Heat Exchanger, *ASHRAE Transactions*, Vol. 82, pp. 289-299.
- Wang, C.C. and Chang, C.T. (1998).** Heat and Mass Transfer for Plate Fin-and-Tube Heat Exchangers, with and without Hydrophilic Coating, *Int. J. Heat Mass Transfer*, Vol. 41, pp. 3109-3120.
- Wang, C.C., Chang, Y.J., Hsieh, Y.C. and Lin, Y.T. (1996).** Sensible Heat and Friction Characteristics of Plate Fin-and-Tube Heat Exchangers Having Plane Fins, *Int. J. Refrigeration*, Vol. 4, pp. 223-230.
- Wang, C.C., Hsieh, Y.C. and Lin, Y.T. (1997a).** Performance of Plate Finned Tube Heat Exchangers Under Dehumidifying Conditions, *J. Heat Transfer*, Vol. 119, pp. 109-117.
- Wang, C.C., Fu, W.L. and Chang, C.T. (1997b).** Heat Transfer and Friction Characteristics of Typical Wavy Fin-and-tube Heat Exchangers, *Exp. Thermal Fluid Sci.*, Vol. 14(2), pp. 174-186.
- Wang, C.C., Chi, K.Y., Chang, Y.J. and Chang, Y.P. (1998).** Experimental Study of Heat Transfer and Friction Characteristics of Typical Louver Fin-and-Tube Heat Exchangers, *Int. J. Heat Mass Transfer*, Vol. 41(4-5), pp. 817-822.
- Wang, C.C., Du, Y.J., Chang, Y.J. and Tao, W.H. (1999c).** Airside Performance of Herringbone Fin-and-Tube Heat Exchangers in Wet Conditions, *Canadian J. Chemical Engineering*, Vol. 77(6), pp. 1225-1230.
- Wang, C.C., Lee, C.J., Chang, C.T. and Lin, S.P. (1999a).** Heat Transfer and Friction Correlation for Compact Louvered Fin-and-Tube Heat Exchangers, *Int. J. Heat Mass Transfer*, Vol. 42, pp. 1945-1956.

- Wang, C.C., Tao, W.H. and Chang, C.J. (1999b).** An Investigation of the Airside Performance of the Slit Fin-and-Tube Heat Exchangers, *Int. J. Refrigeration*, Vol. 22(8), pp. 595-603.
- Wang, C.C., Lin, Y.T. and Lee, C.J. (2000).** Heat and Momentum Transfer for Compact Louvered Fin-and-Tube Heat Exchangers in Wet Conditions, *Int. J. Heat Mass Transfer*, Vol. 43, pp. 3443-3452.
- Webb, R.L. and Trauger, P. (1991).** Flow Structure in the Louvered Fin Heat-Exchanger Geometry, *Exp. Thermal Fluid Sci.*, Vol. 4(2), pp. 205-217.
- Wu, G., and Bong, T.Y. (1994).** Overall efficiency of a straight fin with combined heat and mass transfer, *ASHRAE Transactions*, Vol. 100 (Part 1), pp. 367-374.
- Xia, Y., and Jacobi, A.M. (2004).** An Exact Solution to Steady Heat Conduction in a Two-Dimensional Slab on a One-Dimensional Fin: Application to Frosted Heat Exchangers, *Int. J. Heat Mass Transfer*, 47, 3317-3326.
- Xia, Y., and Jacobi, A.M. (2005).** Air-Side Data Interpretation and Performance Analysis for Heat Exchangers with Simultaneous Heat and Mass Transfer: Wet and Frosted Surfaces, *Int. J. Heat Mass Transfer*, 48, 5089-5102.
- Xia, Y., and Jacobi, A.M. (2010).** A Model for Predicting the Thermal-Hydraulic Performance of Louvered-Fin, Flat-Tube Heat Exchangers under Frosting Conditions, *Int. J. Refrigeration*, 33: 321-333.
- Xia, Y., Zhong, Y., Hrnjak, P.S., and Jacobi, A.M. (2006).** Frost, Defrost, and Refrost and Its Impact on the Air-Side Thermal-Hydraulic Performance of Louvered-Fin, Flat-Tube Heat Exchangers, *Int. J. Refrigeration*, 29:7, 1066-1079.
- Yan, W.M. and Sheen, P.J. (2000).** Heat Transfer and Friction Characteristics of Fin-and-Tube Heat Exchangers, *Int. J. Heat Mass Transfer*, Vol. 43, pp. 1651-1659.